

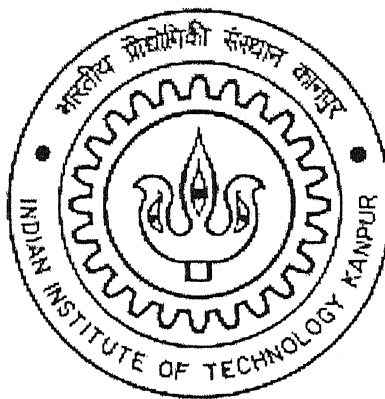
Study of Modification of Flyash Zeolite Using NO_X

*A thesis Submitted
in Partial Fulfilment of the Requirements
for the Degree of*

Master of Technology

by

Roshan G. Shaikh



to the
DEPARTMENT OF CHEMICAL ENGINEERING
INDIAN INSTITUTE OF TECHNOLOGY KANPUR
JULY, 2000

CERTIFICATE

Submitted on 27-7-2018

This is to certify that the thesis entitled "**Study of Modification of Flyash Zeolite Using NO_x**" is the original work of Mr. Roshan G. Shaikh carried out under my supervision and has not been submitted elsewhere for a degree.



(Anil Kumar)

Professor

Department of Chemical Engineering

Indian Institute of Technology

Kanpur-208 016, INDIA

4 OCT 2000 / CHE
CENTRAL LIBRARY
I. I. T., KANPUR
A-131958

TH
CHE 10000/m
Shilp



**Dedicated
To
My Grandmother...**

Abstract

Using flyash waste material, sodium aluminosilicate zeolites have been synthesized with varying Si/Al ratios by a sol-gel process. Using the XRD analysis, these flyash zeolites have been characterized with respect to their molecular structure, geometry of the crystal lattice and Si/Al ratio. These zeolites have also been characterized for their particle size, specific surface area, sorption capacity and the cation exchangeability. These have then been chemically modified using NO_x and we demonstrated the formation of Si- NO_2 bond by the IR, ESCA, XRD and Elemental analysis. The mechanism of nitration reaction of zeolite consistent with experimental observation has been proposed wherein the $-\text{NO}_2$ group is attached to Silicon (Si) atom of zeolite matrix. The XRD studies of the modified and unmodified zeolite show that the crystal structure changes from cubic (100 % crystalline) for the unmodified zeolite to monoclinic (100 % crystalline) for the modified zeolite. The NO_2 group bound to the zeolite has been reduced into an exchangeable ($-\text{NH}_2$) amine group by reaction with hydrazine hydrate. We have found that the anion exchangeability of this amphoteric zeolite increases with its silica content primarily because the nitration occurs on the silica atom alone. In addition to this the cation exchangeability is because of the aluminium atom and is unaltered by the modification reaction. The amine group of flyash zeolite can now undergo organic reaction and in this thesis, we have reacted it with dichloroethane. After quaternization of these with trimethylamine, the anion exchangeability is doubled indicating two dichloroethane molecules have reacted with every amine group of the modified zeolite.

Acknowledgements

I feel pleasure in expressing my most sincere gratitude to **Prof. Anil Kumar** for his valuable guidance and constant encouragement throughout the course of this work. His clear deep insight into my problems, encountered during the period of my work enabled me to accomplish the task. His friendly affection and ever helping attitude made me feel at home at I.I.T. Kanpur. I express my heartiest respect and deepest sense of gratitude.

I sincerely thank all the faculty members of Chemical Engineering Department, whose lectures and guidance helped me in developing the essential capabilities to perform this work.

I express my special thanks to all the staff members of Chemical Engineering Department and ACMS for their kind cooperation.

Inspite of all my interest and industrious efforts, it was not possible for me to take this M.Tech. Programme without the moral support of my friends **Sachin, Sameer and Rahul**. I offer my cordial thanks to them.

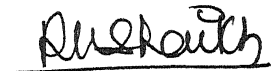
Words can not do full justice in expressing my sincere thanks to my intimate friends **Pankaj, Manoj, Santosh, Sagar, Advait, Lalit, Jitendra and Ramesh** for their splendid company and unforgettable cooperation throughout my stay at I.I.T. Kanpur.

I would like to offer my special thanks to my friends **Anurag and Manish** who have been a ready source of consultation when I needed their unique help.

It is indeed a matter of great pleasure to acknowledge my lab mates **Gaurav, Ritesh, Ashwin, Mishraji, Rajendra, Shankhanilay, Anupam, P. Kumar, sadhana and Arun.**

With the sweet pleasure and respect I remember the love, patience and the sacrifices of all my family members. To them and to all my friends goes the credit for whatever I achieved.

Finally, I pray my prayers to the **One and the Only Strength, the Most Beneficial and Merciful, The Allah, who has created all that exists.**

A handwritten signature in black ink, appearing to read 'Roshan G. Shaikh', written in a cursive style.

(Roshan G. Shaikh)

Contents

List of figures.....	ix
List of Tables.....	x-xii
1. Introduction.....	1-5
2. Experimental Section	
2.1: Pretreatment of Flyash.....	10
2.2: Synthesis of Flyash Zeolite.....	10
2.3: Characterization of Flyash Zeolite.....	11
2.3.1: X-Ray Diffraction (XRD) Analysis	12
2.3.2: Determination of Specific Surface Area.....	12
2.3.3: Scanning Electron Microscopy (SEM).....	13
2.3.4: Determination of Particle Size Distribution.....	13
2.3.5: Determination of Moisture Content & Water Hydration	14
2.3.6 Determination of Cation Exchange Capacity.....	14
2.4: Gas Phase Nitration of Flyash Zeolite using NO _x	16
2.5: Amination of Nitrated Flyash Zeolite.....	17
2.6: Modification of Aminated Flyash Zeolite with Dichloroethane.....	17
2.7: Modification of Chloroethylated Flyash Zeolite with Trimethylamine.....	18
2.8: Determination of Anion Exchange Capacity of Flyash Zeolite.....	18

2.8.1: Regeneration of Anion.....	19
2.8.2: Anion Capacity Determination.....	19
2.9: Synthesis of Mesoporous Silica from TEOS.....	20
2.10: Synthesis of Mesoporous Silica from Flyash Mother Liquor.....	21
3. Results and Discussion	
3.1: Flyash Zeolite Synthesis Process.....	26
3.1.1: Preparation of Fusion Mixture.....	26
3.1.2: Fusion Reaction.....	27
3.1.3: Nucleation of Aluminosilicate.....	27
3.1.4: Alumina Makeup by Sodium Aluminate.....	28
3.1.5: Crystallization Reaction of Flyash Zeolite.....	28
3.2: Synthesis of Flyash Zeolite with Varying Si/Al Ratio.....	29
3.3: Structural Characterization of Flyash Zeolites using X-Ray Diffraction Pattern.....	30
3.4: Surface Area Analysis of Flyash Zeolites.....	32
3.5: Particle Size Distribution of Flyash Zeolite.....	32
3.6: Structural Analysis through Scanning Electron Microscopy (SEM).....	33
3.7: Moisture Content and Water of Hydration of Flyash Zeolite.....	33
3.8: Cation Exchange Capacity of Flyash Zeolite.....	34
3.9: Nitration of Flyash Zeolites.....	34

3.10: Identification of Functional Group through FTIR Analysis.....	35
3.11: Elemental Analysis of Modified Flyash Zeolite.....	36
3.12: Electron Spectroscopy for Chemical Analysis (ESCA)...	36
3.13: Mechanism of Nitration Reaction of Flyash Zeolite.....	37
3.14: Crystallographic Study of Nitrated Flyash Zeolite.....	39
3.15: Anion Exchange Capacity of Modified Zeolite.....	40
3.16: Anion Exchangeability of Quarternized Flyash Zeolite....	40.
3.17: Characterization of Mesoporous Silica.....	41
3.18: Modification of Mesoporous Silica using NO _x	42
3.19: Analysis of Functional Groups through FTIR Analysis....	42
3.20: Anion Exchangeability of Modified Mesoporous Silica...	42
4. Conclusion.....	66
5. References.....	68

List of figures

Figure 2.1: Reactor used for nitration reaction	23
Figure 3.1: SEM photographs of flyash zeolite (A-4) and standard zeolites.....	44
Figure 3.2: Photograph of (a) Blank (b) Nitrated and (c) Aminated flyash zeolite (A-4).....	45
Figure 3.3: FTIR spectra of (a) Blank (b) Nitrated and (c) Aminated flyash zeolite	46
Figure 3.4: FTIR spectra of (a) Dichloroethane modified (b) Trimethylamine quarternized flyash zeolite.....	47
Figure 3.5: ESCA spectra of Si 2p binding energy for the blank and modified (a) Silica gel and (b) Quartz sand in the 105 –145 eV range.....	48
Figure 3.6: ESCA spectra of Si 2p binding energy for the blank and modified (a) Silica gel and (b) Quartz sand in the 150 – 190 eV range.....	49
Figure 3.7: ESCA spectra of N1s binding energy for Modified (a) Quartz sand and (b) Silica gel.....	50
Figure 3.8: Comparative XRD pattern of modified and unmodified flyash zeolite (A-4).....	51
Figure 3.9: Photographs of (a) Blank (b) Nitrated and (c) Aminated mesoporous silica.....	52
Figure 3.10: FTIR spectra of (a) Blank (b) Nitrated and (c) Aminated mesoporous silica	53

List of Tables

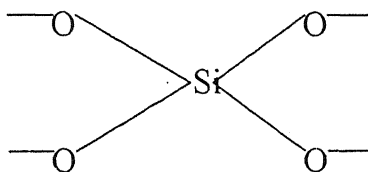
Table 1.1: Typical commercially available aluminosilicate zeolites.....	6-8
Table 1.2: Report on the doing of microporous and mesoporous materials with variety of metals.....	9
Table 2.1: Optimal conditions and molar compositions for the synthesis of flyash zeolite A/Y.....	24
Table 2.2: Chemical formulations and optimal conditions used For the synthesis of mesoporous silica.....	25
Table 3.1: Chemical formulations and process conditions used for the synthesis of flyash zeolites with varying silica alumina content.....	54
Table 3.2: Comparative XRD values of flyash zeolites and its most closely matching Na-aluminosilicate zeolite chosen from JCPDS cards.....	55-57
Table 3.3: Structural characterization of flyash zeolites and standard zeolites using XRD analysis.....	58
Table 3.4: Particle size distribution of flyash zeolites and standard zeolites.....	59
Table 3.5: Moisture Content and the water of hydration of flyash zeolites and standard zeolites.....	60
Table 3.6: Cation exchange capacity of flyash zeolites and standard zeolites...	61
Table 3.7: Details of experimental conditions of nitration reaction and analysis of number equivalents of nitrogen attached per repeat unit of flyash zeolite.....	62
Table 3.8: d-spacing and relative intensity values of XRD analysis for flyash zeolite A-4 & nitrated zeolite A-4 and their most closely matching	

standard zeolite reported in the JCPDS cards.....	63
Table 3.9: Anion exchange capacity of aminated and quarternized flyash zeolite.....	64
Table 3.10: The characterization of mesoporous silica synthesized from TEOS and flyash mother liquor.....	65

CHAPTER 1

INTRODUCTION

Aluminosilicate zeolites are microporous crystalline inorganic polymer containing well-defined cavities and channels of molecular dimensions. The cavities and channels are precisely uniform in size and these pores can accept molecules of certain size while rejecting molecules of larger dimension. In view of this, these molecules are also known as molecular sieves. The primary building block of aluminosilicate zeolite structure is a tetrahedron comprising of four oxygen atoms surrounding a central silicon atom (SiO_4)⁴⁻ and can be represented by



Primary building unit

These tetrahedrons are connected through shared oxygen atoms to form a wide range of secondary building units. Different combinations of these secondary units give rise to numerous distinctive zeolites framework structure with varying pore size.

The Si / Al ratio can range from the minimum value of 1 to a maximum of about 500. International Zeolite Association has assigned a special three letter code nomenclature to zeolite and some of these are given in Table 1.1^(1,2,44,45). The FAU zeolite represents the family of material with faujasite-type structure. Many materials are more commonly known by the

names of the laboratories in which they were discovered. Pore size varies from about 2.5 Å in case of sodalites (SOD-containing six tetrahedron in largest channel) to about 10 Å in so-called UTD-1, which contains 14 tetrahedrons in the largest channel³. The majorities of open framework system with large channels contain rings with even number of tetrahedron sites i.e. 6-, 8-, 10-, 12-, or 14 rings but there are evidences for both 7- and 9- rings in high silica zeolites SSZ-23⁴.

Inorganic polymers can generally be classified based on the size of pores into macroporous (pore size > 500 Å), microporous (pore size < 20 Å) and mesoporous (pore size 20-100 Å). These mesoporous materials have pore size of 20-100 Å, considerably larger than microporous zeolite. These mesoporous inorganic polymers have extremely high specific surface area (>1000 m²/g) and large pore size, which made this material highly interesting.

The mesoporous inorganic polymers are synthesized by liquid templating mechanism, which is also known as sol-gel process. In the sol-gel process, surfactant is used as structure directing agent. One of the many mechanisms proposed to explain the formation of the large pore framework is that, soluble form of the inorganic species in the reacting gel are guided by surfactants. These surfactant molecules aggregate themselves to form micelles, which interact with inorganic species in the solution and get surrounded. This leads to the formation of inorganic mesopores⁵. During the calcination of the product, which is carried out after the sol-gel reaction, surfactants in the micelles are burnt leaving behind an open pore framework.

Alkyl-tri-methyl ammonium bromide having molecular structure of $C_nH_{2n+1}(CH_3)_3NBr$ is the most common surfactant used. It was found that the nature of the product, whether it is microporous or mesoporous, depends upon the alkyl chain length (n) of this molecule⁶.

Mesoporous materials with high specific surface area and large pore openings have been shown to play a vital role in catalysis and adsorption⁵. The organic functional groups needed for catalysis and adsorption are grafted onto the surface of these inorganic supports through functionalization. Functionalized material has ill defined size, shape and low crystallinity due to these attached functional groups⁷. In the literature, functionalization has been achieved by sol-gel process in which, molecules having the required functional groups are trapped in the framework. However this leads to more disordered structure and non-uniform pore size distribution⁸. Inagaki et al⁷. through sol-gel polymerization attached ethane fragments ($-CH_2-CH_2-$), methylene ($-CH_2-$), phenylene ($-C_6H_4-$) and vinylene ($-CH=CH-$) onto the structure of the mesoporous silica. A catalytically active metal cation can be included into the framework formed in sol-gel reaction by Doping. The incorporation of dopant into the silicates or any inorganic framework depends upon cation size and coordination state of dopant⁵. According to the Pauls theory⁹ of chemical bonding, the metal dopant is coordinated tetrahedrally by four oxygen atoms, when the ratio of radii of dopant cation and oxygen anion slightly exceeds 0.414. The incorporation is also found to be dependent upon the pH of the synthesis mixture. Table 1.2⁽¹⁰⁻

³⁷⁾ gives a report on the doping of microporous and mesoporous materials with variety of metals.

After the zeolite is formed by the sol-gel process, its further modification has been done using trialkoxy silane compounds. The metal sorbent, which has great affinity for Zn^{++} and Cu^{++} , is prepared by anchoring trimethoxy amino propyl silane to hexagonally packed mesoporous silica³⁸. Beck et al.³⁹ has introduced carboxylic acid group onto the surface of MCM-41 by reacting (3-trimethoxysilyl) propyl succinic anhydride with tetraethylorthosilicate (TEOS) in the alkaline medium. Liu et al.⁴⁰ treated hexagonal mesoporous material with phenanthroline Iron (II) chloride. The resulting material is found to possess excellent catalytic activity for oxidation of phenol with H_2O_2 as oxidant. Sutra and Brune et al.⁴¹ has functionalized MCM-41 material with Manganese–triazacyclononane complex that served as epoxidation catalyst for styrene and cyclohexane. The catalyst for the oxidation of olefin is prepared by the encapsulation of Ruthenium Porphyrins in MCM-41 material. This catalyst is found to possess 20-40 times more catalytic activity than Porphyrin without this support material⁴². The MCM-41 material with cobalt oxide species anchored to its surface showed good catalytic property for selective oxidation of cyclohexane to cyclohexanone⁴³. Mehnert et al.⁵ prepared the catalyst needed for ethylene polymerization by attaching Zirconocene complex onto the surface of mesoporous silica through their siloxy group.

In the present work, the modification of flyash zeolite has been carried out by gas phase nitration using a mixture of NO and NO₂ called as NO_x. This scheme of modification introduces the nitro group (-NO₂) in the zeolite framework, which is subsequently converted into exchangeable amine group (-NH₂) by amination using hydrolyzed hydrazine. The Na-zeolites with varying Si/Al ratio have been synthesized through sol-gel polymerization using flyash as silica-alumina source. This has been done so, in order to utilize a solid waste material for the ecological purposes. We have also procured the commercially available sodium aluminosilicate zeolites for the standardization of our flyash zeolite. The flyash based Na-zeolite has a cation exchange capacity comparable with commercial zeolite. The amine group (-NH₂) introduced by modification with NO_x has been found to have ability to get exchanged with other anions and can be regenerated using the standard procedure. Thus, the flyash zeolite prepared by us is converted into an amphoteric exchanger through modification. The anion exchange capacity of this zeolite is comparable with commercially available organic polymer based anion exchanger material. The anion exchangeability of aminated zeolite gets nearly doubled when it is modified with dichloroethane and subsequently quarternized with trialkyl amine compounds.

Structure Type	Natural/Synthetic	Unit cell composition	Si/Al ratio	Exchange cations	Pore system	Pore Diameter Å°
Zeolite-A (LTA)	Natural ZK-4, ZK-5, No mineral analogue	$\text{Na}_{12}(\text{AlO}_2)_{12}(\text{SiO}_2)_{12}$	1.0	K^+ , Ca^{++} , Na^+	3-Dimensional 8-Ring Channel	4.2
Zeolite-X (FAU)	Synthetic Zeolite-X, No mineral analogue	$\text{Na}_{86}(\text{AlO}_2)_{86}(\text{SiO}_2)_{106}$	1.0-1.5	Na^+	3-Dimensional 8-Ring Channel	7.4
Zeolite-Y (FAU)	Synthetic Zeo-Y, US-Y, Mineral –FAU	$\text{Na}_{56}(\text{AlO}_2)_{56}(\text{SiO}_2)_{136}$	1.5-3.0	Na^+	3-Dimensional 12-Ring channel	7.4
Mordenite (MOR)	Synthetic	$\text{Na}_8(\text{AlO}_2)_8(\text{SiO}_2)_{40}$	5.0	Na^+	3-Dimensional 12-Ring Channel	6.7 x 7.0
Erionite (ERI)	Natural	$(\text{Ca}, \text{Mg}, \text{K}_2, \text{Na}_2)_{4.5}$	3.0-3.5	K^+ , Ca^+ , Na^+ , Mg^{++}	3-Dimensional 8-Ring Channel	3.6 x 5.2
Zeolite - L (LTL)	Synthetic	$\text{K}_9(\text{AlO}_2)_9(\text{SiO}_2)_{27}$	2.6	K^+	1-Dimensional 6-Ring Channel	7.1
Sodalite (SOD)	Natural as well as synthetic	$3\text{Na}_2\text{O}: 3\text{Al}_2\text{O}_3: 6\text{SiO}_2$	1.0	K^+ , Na^+	3-Dimensional 6-Ring Channel	2.5
Ferrierite (FER)	Natural as well as synthetic	$(\text{K}^+, \text{Na}^+)(\text{AlO}_2)_8(\text{SiO}_2)_{40}$	5.0	K^+ , Na^+	3-Dimensional 12-Ring Channel	6.7
Chabazite (CHA)	Natural as well as synthetic	$(\text{K}^+, \text{Na}^+)(\text{AlO}_2)_1(\text{SiO}_2)_2$	5.0	K^+ , Na^+	3-Dimensional 8-Ring Channel	3.9
ZSM-4 (MFI)	Synthetic	$(\text{TMA}, \text{Na})_x(\text{AlO}_2)_x(\text{SiO}_2)_y$ $y/x = 5.0-10.0$	5.0-10.0	TMA, Na^+	-	-
ZSM-5 (MEL)	Synthetic	$(\text{Cation})_x(\text{AlO}_2)_x(\text{SiO}_2)_y$ $y/x = 6.0-50.0$	6.0-50.0	TPA or Na^+	3-Dimensional 10-Ring Channel	5.1 x 5.8
ZSM-11 (MFI)	Synthetic	$(\text{Cation})_x(\text{AlO}_2)_x(\text{SiO}_2)_y$ $y/x = 10.0-45$	10.0-45	TBP, TBA	1-Dimensional	5.3 x 5.4

Table 1.1: Typical commercially available aluminosilicate zeolite

Structure type	Natural/Synthetic	Unit cell composition	Si/Al ratio	Exchange cations	Pore system	Pore diameter \AA°
ZSM-35 (FER)	Synthetic	$(\text{Cation})_x(\text{AlO}_2)_x(\text{SiO}_2)_y$ $y/x = 4.0-25.0$	4.0-25.0	ED, P, Na^+	1-Dimensional	-
ZSM-20 (FAU)	Synthetic	$(\text{Cation})_x(\text{AlO}_2)_x(\text{SiO}_2)_y$ $y/x = 3.5-5.0$	3.5-5.0	TEA, Na^+	1-Dimensional	4.4 x 5.5
ZSM-21 (FER)	Synthetic	$(\text{Cation})_x(\text{AlO}_2)_x(\text{SiO}_2)_y$ $y/x = 4.0-25.0$	4.0-25.0	ED, P, C, Na^+	1-Dimensional	4.5 x 5.2

Table 1.1: Typical commercially available aluminosilicate zeolite

Code	Full Name
LTA :	Linde Type A
FAU :	Faujasite
CHA:	Chabazite
ERI :	Erionite
LTL :	Linde Type L
MOR:	Mordenite
MEL :	ZSM-11
MFI:	ZSM-5
TMA : $(\text{CH}_3)_4\text{N}^+$	Tetramethyl ammonium
TEA : $(\text{C}_2\text{H}_5)_4\text{N}^+$	Tetraethyl ammonium
TPA : $(\text{C}_3\text{H}_7)_4\text{N}^+$	Tetrapropyl ammonium
TBA : $(\text{C}_4\text{H}_9)_4\text{N}^+$	Tetrabutyl ammonium
TBP : $(\text{C}_4\text{H}_9)_4\text{P}^+$	Tetrabutyl Phosphine
ED : $\text{NH}_2\text{-CH}_2\text{-CH}_2\text{-NH}_2$	Ethylene diamine
C : $(\text{CH}_3)_3\text{N-CH}_2\text{-CH}_2\text{-OH}$	Choline

Structure type designation used in table 1.1

Sr. No	Metal cation	$r [M^{n+}] / r [O_2]$	Structure	pH of synthesis mixture	Ref. No
1.	Titanium (Ti^{4+})	0.486	ZSM-5	Alkaline	10
			ZSM-11	Alkaline	10
			MCM-41	Alkaline	11
			MCM-48	Alkaline	12
2.	Vanadium (V^{4+})	0.421	ZSM-5	Alkaline	10
			ZSM-11	Alkaline	10,13
			ZSM-48	Alkaline	10,14
			MCM-48	Acidic; Neutral	15
			MCM-41	Alkaline	16
3.	Chromium (Cr^{3+})	0.457	ZSM-5	Alkaline	17,18
			ZSM-11	Alkaline	17,18
			MCM-48	Alkaline	15
			MCM-41	-	19
4.	Manganese (Mn^{2+})	0.571	MCM-41	Alkaline	20
			MCM-41	Acidic; Neutral	19
5.	Ferrous (Fe^{3+})	0.457	ZSM-5	Alkaline	21
			ZSM-11	Alkaline	21
			MCM-41	Neutral	22
			MCM-48	Alkaline	23
6.	Cobalt Co^{2+}	0.514	ZSM-5	Alkaline	24
7.	Copper Cu^{2+}	0.514	ZSM-11	Alkaline	26
8.	Zinc (Zn^{2+})	0.529	ZSM-5	Alkaline	27
			FAU-Y	Alkaline	28
9	Zirconium Zr^{4+}	0.571	ZSM-5	Alkaline	29
10	Tin (Sn^{4+})	0.507	ZSM-5	Alkaline	30
			ZSM-11	Alkaline	30,31
			MCM-41	Neutral	32
11	Arsenic (As^{5+})	0.35	ZSM-5	Alkaline	33
12	Molybdenum	-	MCM-41	Acidic; Neutral	19
13	Niobium (Nb)	-	MCM-41	Alkaline	34
14	Boron (B)	-	MCM-41	Basic, neutral	22,35
15	Gallium (Ga)	-	MCM-41	Basic, Neutral	22,36
16	Aluminum (Al^{3+})	-	MCM-41	Alkaline	37

Table 1.2: Report on the doping of microporous and mesoporous material with variety of metal cations.

Chapter 2

Experimental Section

The sodium aluminosilicate zeolites could be prepared from flyash by following the steps given below.

2.1 Pretreatment of flyash

Flyash needed for the synthesis of zeolite is collected locally from Panki Thermal Power Station, Kanpur. This contains unburned carbon and iron, which are undesirable for zeolite synthesis and must be removed. For doing so, flyash is first sieved using a 53-micron mesh screen. The carbon particles are removed by ashing and flotation technique. Iron is removed first by magnetic separation followed by acid treatment, which is done by refluxing the flyash (100 g) with hydrochloric acid (AR HCl, 8N) for 4 hours at about 105 to 110 °C. The treated flyash is then washed with distilled water till all acidity is removed (as checked by pH paper) and dried in an oven maintained at 100-110 °C. This acid treated flyash is now ready for the zeolite synthesis. The elemental analysis of this flyash is determined using Electron Probe Micropore Analyzer (EPMA). This analysis shows that, it contains 58% Silicon, 38.5 % Aluminum and 3.5 % Iron.

2.2 Synthesis of Flyash Zeolites

The acid treated flyash (20 g) is ground with caustic soda pellets (24 g) in the ratio 1:1.2 to obtain a fine homogeneous material called fusion mixture. The alkali is used in excess in order to maintain pH of 12 to 12.5 during the reaction. Proper grinding of fusion mixture avoids the formation of

glassy phase during the fusion as discussed below, which forms the sodium silicates. The fusion mixture is kept at 700°C in a muffle furnace for 2 hours to obtain a fused mass (45 g). After this, it is cooled, milled, and kept for agitation by mixing with distilled water (200 ml) in the ratio of 1:4. The Agitation of 8-10 hours is found to be sufficient for the formation of nuclei of aluminosilicates. After the nucleation, the silica and alumina content is adjusted properly as follows. The 15% Sodium aluminate solution is added into the slurry as alumina makeup for zeolite-A synthesis. For zeolite-Y synthesis, no alumina is required because alumina needed for it, is present in the flyash itself. Then the slurry is subjected to hydrothermal crystallization reaction at 105°C in an autoclave. Table 2.1 shows the optimal condition and the molar compositions for the synthesis of flyash zeolite-A/Y. After the crystallization, the solid product is filtered and the mother liquor is separated. The crystalline aluminosilicate is washed thoroughly with distilled water to remove all alkalinity as checked by pH paper. The solid product is dried in an oven maintained at 105°C to get required flyash zeolite.

2.3 Characterization of Flyash Zeolites

The flyash zeolites so synthesized are characterized with respect to the following

1. X-Ray Diffraction pattern (XRD)
2. Specific surface area (m^2/g)
3. Scanning electron microscopy (SEM)
4. Particle size distribution
5. Moisture content and water of hydration.

6. Cation exchange capacity in meq. /g (CEC)
7. Infra-Red spectroscopy (IR)
8. Elemental analysis.

2.3.1 X-Ray Diffraction Pattern (XRD)

Powder XRD analysis is employed to monitor zeolite formation process using X-Ray Powder Diffractometer, which uses Cu K α as source of X-Ray (Model Isodevyeflux 2002, made by Rich Seifert & Co, West Germany). During all XRD analysis, the X-Ray wavelength is kept constant at 1.5406 \AA and the relative intensity of the diffraction is recorded as the function of 2θ . The d-spacing value of standard zeolite sample reported in JCPDS file formed the basis for the comparison.

2.3.2 Determination of Specific Surface area

The specific surface area of the powder zeolite is determined by BET Surface area analyser (Model No. SA-3100, Coulter Company, England). This instrument works on a simple principle of BET isotherm adsorption. The surface area of the zeolite is determined by following relation.

$$S = V_m A (N / M)$$

In this relation, V_m is the volume of gas at STP required to form an adsorbed monomolecular layer, A is the Avogadro's number which expresses the number of gas molecules present per mole of the gas at the standard conditions of temperature and pressure, M is the molar volume of the gas and N is the area of each adsorbed gas molecule in m^2 . Measurement of surface area is done by passing the carrier gas in the ratio of 30 % N_2 and 70 % He

through the sample. The nitrogen is used as an adsorbate gas and helium is the carrier gas. The sample holder is immersed in the liquid nitrogen bath at a very low temperature (-197°C) at which nitrogen gas gets condensed and is adsorbed onto the surface of the zeolite. The above instrument uses the ready-made software, which does all calculations and reports the specific surface area of zeolite in m^2/g

2.3.3 Scanning Electron Microscopy (SEM)

The structural morphology of flyash zeolite is examined by Jeol-840-A Scanning electron microscope (SEM).

2.3.4 Determination of Particle Size Distribution

The particle size analysis of powder zeolite sample is carried out with Laser particle size analyzer, (Model Fritsch Economy, Fritsch GMBH, Germany). This instrument works on the principle that the scattering of the laser beam depends upon the size of particles. The low concentration suspension of zeolite is prepared by adding a small amount of it into the distilled water. The suspension is continuously stirred (65 rpm) and subjected to the ultrasonic vibrations (65 unit), in order to break the lumps and keep each particle well dispersed. The laser beam of fixed intensity is passed through this suspension and the instrument records the change in intensity of laser beam due to the scattering. The instrument has been equipped with ready-made latest software, which carries out all the analysis, and gives the particles size distribution of zeolites on the cumulative percentage basis.

2.3.5 Determination of Moisture content and Water of Hydration

Approximately 1 g of air-dried sample is weighed accurately designated as W_1 and kept for oven drying to remove its moisture content at 110°C for 2 hours and designated as W_2 . The difference between W_1 and W_2 is expressed as percent moisture content. The same sample is subjected to furnace heating at 800°C for 2 hour. After cooling it to room temperature, the sample is weighed again and is designated as W_3 . The difference between W_2 and W_3 gives the loss of Water of Hydration on ignition. It is reported in terms of Percent Water of Hydration on the oven dry basis using following relation

$$\% \text{ Moisture Content} = \frac{W_1 - W_2}{W_1} \times 100 \longrightarrow 2.3.5.a$$

$$\% \text{ Water of Hydration} = \frac{W_2 - W_3}{W_2} \times 100 \longrightarrow 2.3.5.b$$

2.3.6 Determination of Cation Exchange capacity (CEC)

The cation exchangeability of flyash zeolite is determined as follows 0.5 g of hydrated calcium chloride is dissolved in 1.1 litre of distilled water and pH is adjusted at 9-9.5 with dilute sodium hydroxide solution. Approximately 100 ml of this Ca^{++} solution is taken out for the analysis of Ca^{++} content. Approximately 1.0 g of oven-dried zeolite is mixed and stirred with rest of (approximately 1000 ml) of Ca^{++} solution for 1 hour at room temperature. After the filtration, filtrate is collected and exhausted sodium zeolite is kept for regeneration by treating with 10 percent sodium chloride solution. After this, the Ca^{++} content of original solution and filtrate is determined by the standard

procedure⁴⁶. From the difference between Ca^{++} concentration of original solution and filtrate, the cation exchange capacity is calculated as mequivalent per gram of oven-dry zeolite.

The concentration of calcium ions in the solution is determined by taking 50 ml of the sample in titration flask. pH of the sample is adjusted at 10.0 by adding dilute sodium hydroxide solution. Approximately 0.1 to 0.2 g of ammonium purpurate indicator is added to this sample. (Ammonium purpurate indicator is prepared by grinding the mixture of murexide (0.2 g) and NaCl (100 g) to 40-50 mesh size.) This is then titrated against 0.01 M ethylenediamine tetra acetic acid (EDTA) solution with end point change sharply from pink to purple. 2-3 drops of titrant is added in excess in order to make it certain that, no further colour change occurs. The cation exchange capacity of zeolite is found by following relation

$$\text{Cation exchange capacity (Meq. /g)} = \frac{(A - B)}{C \times D} \times 20 \quad \longrightarrow 2.3.6.a$$

Where,

A = ml of 0.01M EDTA solution consumed for original calcium ion solution.

B = ml of 0.01M EDTA solution consumed for exchanged calcium ion solution.

C = ml of sample taken for titration.

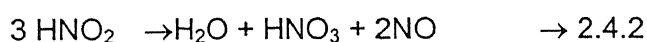
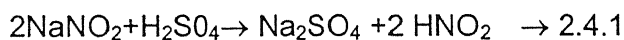
D = Mass of oven dry zeolite taken for exchange (grams)

The result of exchanging sodium zeolite with calcium ions is the formation of calcium zeolite. Mixing with 10 percent sodium chloride solution for 1 hour converts this Ca-zeolite into the Na-zeolite. The cation exchange

capacity of this regenerated zeolite is determined by the same procedure discussed above

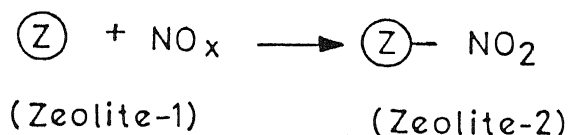
2.4 Gas phase nitration of zeolite using NO_x

Direct gas phase nitration of zeolite is carried out in a three-litre reaction bottle shown in figure 2.1. The lid of this reaction vessel is made-up of steel and is equipped with a brass cap with 1.2 mm opening at the top for injecting the gas, which is sealed by the silicon rubber septum. Double neck round bottom flask is used to produce NO_x. The NO_x is produced by reacting sodium nitrite NaNO₂ (10, g mole) with sulfuric acid (H₂SO₄ sp. gr. 1.98, 25ml) in ferrous sulfate FeSO₄ (1, g mole). One neck of the flask is closed with rubber septum for withdrawing gas with the 100-ml syringe. The generation of NO_x occurs through the following mechanism



Approximately 15 g of the air-dry sample of zeolite is taken in the reaction vessel. The vacuum is created inside the vessel by vacuum pump. Vacuum must be such that when NO_x gas is introduced into the reaction bottle, at the reaction temperature, the total pressure should not exceed the atmospheric pressure to avoid leakages. The nitration reaction in a single run is carried out at 225 °C in an oven for about 18 hours. Then reaction vessel is cooled, and water formed in reaction, which is found to adhere to the wall of

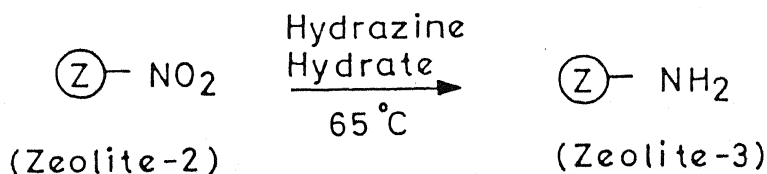
vessel is cleaned. More set of nitration is carried out till zeolite become saturated for any more consumption of NO_x . Small amount of the sample is taken out for characterization and the rest of the material is now ready for the amination reaction. Approximately 1000 CC of NO_x is consumed per gram of air-dry zeolite.



Where Z represents the single matrix of zeolite structure.

2.5 Amination of Nitrated Flyash Zeolite

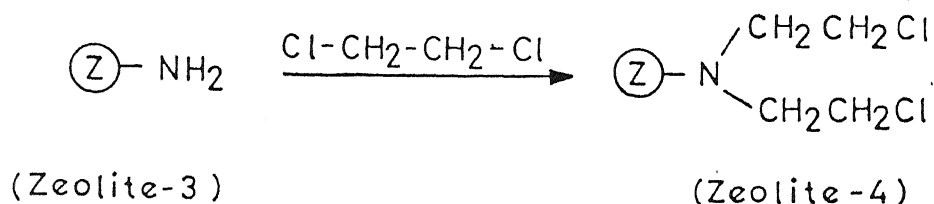
Amination of nitrated zeolites are carried out with hydrazine hydrate. About 12 g of sample is taken in flat bottom reflux flask along with 100 ml (50 %) hydrazine hydrate. The reaction mass is refluxed for 4 hours at 65 °C in water bath, which is maintained at 70 °C. The solid product is washed thoroughly with distilled water and dried in an oven at 100 °C. This aminated zeolite is ready for further modification reaction. Small sample is taken out for characterization and the rest of the material is kept for modification. The anion exchange capacity of aminated zeolite is found out by standard procedure described in section 2.8. The reaction takes place is as follows



2.6 Modification of Aminated Flyash Zeolite with Dichloroethane

Approximately 10 g of aminated zeolite is refluxed with 100 ml of 10% (by volume) solution of dichloroethane in ethanol for 4 hours at 65 °C.

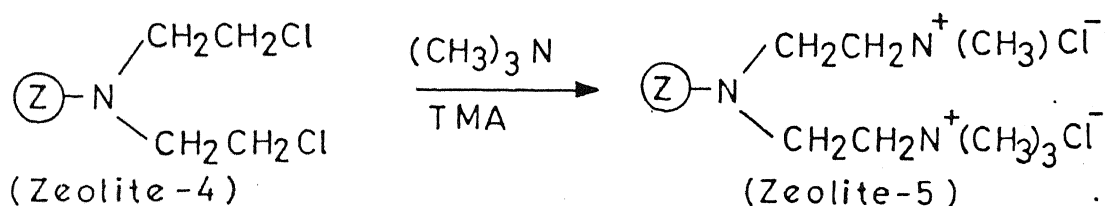
After the completion of the reaction, the zeolite is filtered, washed, and dried in an oven at 100 °C. Higher concentration of dichloroethane is avoided because, zeolite becomes sticky and lumps are formed. The reaction occurred as follows



Above Z represent a single matrix of zeolite. This modified zeolite is easily quarternized using trimethylamine as described below.

2.7 Modification of Chloroethylated Zeolite with Trimethylamine

After the modification of zeolite with dichloroethane, the oven dried chloroethylated zeolite is refluxed with 100 ml of 6 percent solution in ethanol at 65 °C for 4 hours. After the completion of the reaction, the product is washed and dried. The anion as well as the cation exchange capacity of this quarternized zeolite is determined. The reaction occurring during this modification is as follows.



2.8 Determination of Anion Exchange Capacity of Zeolite

The exchange capacity of aminated as well as quarternized zeolite is determined using gravimetric method given in ASTM standard number ASTM D 2187, 2687, 3087, 3375, and ISI). It involves following steps

2.8.1 Regeneration of Anion

In this first mixed acid is prepared by mixing 18.1 ml of H_2SO_4 (sp.gr.1.84) with 27.5 ml of HCl (sp.gr.1.19) in 500 ml of distilled water. The entire content is made up to 1000 ml using distilled water. After this, the test water is prepared by diluting the mixed acid by distilled water up to 1 percent concentration. This test water is then added to the modified zeolite in a quantity of 100 ml per gram of and kept for 24 hours. After this, the zeolite is filtered and washed with distilled water till all acidity is removed as checked by litmus paper.

2.8.2 Anion capacity determination

The anion regenerated modified zeolite is kept in 0.1 N NaNO_3 solution for 24 hours. Then the reaction mass is filtered. Approximately 1.7 g AgNO_3 is added to the filtrate and 2-3 drops of concentrated HNO_3 is added to bring the pH of the solution to 2.0. The entire content is again kept for 24 hours. The chloride ion present in the filtrate forms AgCl , which appears as white precipitate. The precipitate is filtered and weighed. The anion exchange capacity of modified zeolite is calculated using the following relation.

$$\text{Anion exchange capacity (Meq. / g)} = \frac{W_1}{M}$$

Where,

W_1 = Oven dry mass of silver nitrate precipitate.

M = Molecular weight of silver nitrate.

2.9 Synthesis of Mesoporous Silica from TEOS

We have also synthesized the mesoporous silica starting from tetraethoxyorthosilicate (TEOS) by adopting the following procedure. Approximately 700 ml of distilled water is taken in the high-pressure autoclave reactor and about 9.5 g of NaOH pellets is added to it, in order to bring the pH of solution to 9.8–10.0. Approximately 75 ml of triethoxyorthosilicate is added to this solution. Then 10–12.7 g of cetyltrimethyl ammonium bromide (CTAB) is added with constant stirring in order to mixed it completely in the reaction mass. This surfactant acts as a structure-directing agent. Then the autoclave reactor is closed and kept for the heating at constant temperature of 160 °C with constant stirring for about 24 hours. At this temperature mesoporous silica starts precipitating in the crystalline form from TEOS solution. After 24 hours, the reactor is cooled to room temperature and solid product is washed thoroughly with distilled water to remove all the surfactant adhering on the surface of the formed mesoporous silica. Then it is dried in an oven at 65 °C and subsequently subjected to the calcination at 520 °C in a muffle furnace. Calcinations is employed to burn the surfactant micelles which are present in the pores of the silica framework. This gives an open-pore framework mesoporous silica. After cooling it to the room temperature, its yield is calculated by weighing the mass of the product. Table 2.2 shows the chemical formulation and optimal conditions optimal conditions used to synthesize mesoporous silica.

2.10 Synthesis of Mesoporous Silica from the Flyash Mother Liquor

We have also synthesized the mesoporous silica by sol-gel process from flyash used as silica source. The silica present in the flyash is in the solid form and it is absolutely insoluble in water. The silica in its source material must be present in the dissolved form so that it can be guided easily by the surfactant molecules in the liquid medium. In the zeolite synthesis, after crystallization reaction, the mother liquor was collected from the reactor, which contains silica in the form of soluble sodium metasilicate.

Approximately 500 ml of distilled water is taken in autoclave reactor and about 250 ml of mother liquor is added to it with stirring. This mother liquor is highly alkaline (pH 12.5) hence 0.1 N, sulfuric acid (approximately 15 ml) is added to this solution in order to bring the pH of solution to about 9.8–10.0 at which silica gets precipitated. The cetyltri-methyl ammonium bromide surfactant (approximately 12.5 g) is added to this, which acts as a structure-directing agent. Then the autoclave is closed and kept for heating at a constant temperature of 175 °C with constant stirring for about 12 hours. At this temperature mesoporous silica starts precipitating in the crystalline form from the mother liquor. After 24 hours, the reactor is cooled to room temperature and solid product is washed thoroughly with distilled water to remove all the surfactant adhering on the surface of the formed mesoporous silica. Then it is dried in an oven at 65 °C and subsequently subjected to the calcination at 600 °C in a muffle furnace. Calcinations is employed to burn the surfactant micelles which are present in the pores of the silica framework. This gives an open-pore framework mesoporous silica. After cooling it to the room

temperature, its yield is calculated by weighing the mass of the product. Table 2.2 shows the chemical formulation and optimal conditions used to synthesize mesoporous silica.

We have characterized these mesoporous silica with respect to surface area, pore volume, XRD and particle size. Then we have carried out the modification and determined its anion exchangeability.

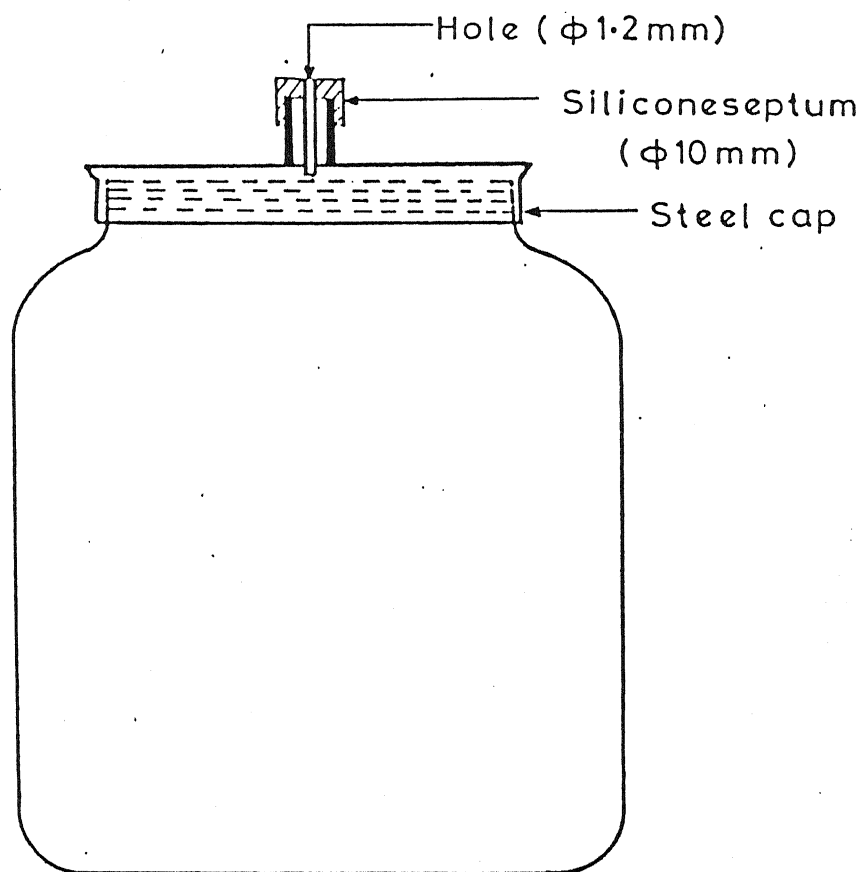


Figure 2.1: Reactor used for nitration of flyash zeolite.

(I) Molar compositions of different species during flyash zeolite A and Y Synthesis			
Sr. No	Molar composition	Experimental ratio	
		Zeolite-A	Zeolite-Y
1	SiO ₂ /Al ₂ O ₃	1.71	3.45
2	Na ₂ O/ SiO ₂	2.30	1.50
3	H ₂ O/ Na ₂ O	26.52	37.0
<ul style="list-style-type: none"> flyash is used as Alumina and silica Source Sodium aluminate is used as makeup alumina source for zeolite-A 			
(II) Optimal conditions for synthesis of flyash zeolite A and Y.			
Sr. No	Parameters	Flyash zeolite-A	Flyash zeolite-Y
1	Flyash / NaOH ratio	1:1.2	1:1.2
2	Sodium aluminate	4.0 – 6.0 g	0.0 g
3	Fusion temperature	700 °C	700 °C
4	Nucleation time (hours)	8.0 – 10.0	8.0 – 10.0
5	Crystallization time (hours)	3 -4	8 - 10

Table 2.1: Optimal conditions and molar compositions for the synthesis of flyash zeolite A and Y

Sr. No.	Name of sample	Silica source	Surfactant amount	pH	Alkali/Acid	Water ml	Reaction temperature °C	Reaction time	Calcination temperature (°C)	Yield (Grams)
1	Meso-Si-1	TEOS 75 ml	12.7 g	9.8	NaOH 9.5 g	700	160	24 hours	520 (5 hours)	35 grams
2	Meso-Si-2	TEOS 75 ml	10.0 g	9.8	NaOH 9.5 g	700	160	24 hours	520 (5 hours)	32 grams
3	Flyash meso-Si	Mother liquor 250 ml	12.5 g	9.8	H ₂ SO ₄ 0.1 N (15 ml)	500	175	12 hours	600 (3 hours)	5 grams

- Surfactant used is Cetyl trimethyl ammonium bromide powder
- Mother liquor is obtained from the crystallization reaction of flyash zeolite (A – 1) synthesis.
- H₂SO₄ (0.1 N) is used because flyash mother liquor is highly alkaline

Table 2.2: The chemical formulations and optimal conditions used for the synthesis of mesoporous silica.

Chapter 3

Results and Discussion

3.1 Flyash Zeolite Synthesis Process

The synthesis of zeolite in general is a simple process and its procedure of preparation from flyash involves the following five major steps

1. Mixing and grinding of acid treated flyash (Consisting of free silica and alumina) with sodium Hydroxide pellets in the completely dry condition. This gives the fusion mixture.

2. Fusion reaction gives a mixture of sodium silicates and sodium aluminate called as fused mass.

3. Agitation of the slurry of this fused mass after mixing it with distilled water in the ratio of 1:4. This facilitates the nucleation of aluminosilicate zeolite.

4. The alumina content of this nucleated slurry is made up with sodium aluminate solution.

5. The crystallization of this aluminosilicates zeolite under autogenous hydrothermal pressure (1.3 atm.) at 105 °C.

3.1.1 Preparation of Fusion Mixture

The acid treated flyash is first dried and then ground with sodium hydroxide pellets in the ratio of 1:1.2 under the absolute dry condition in a grinder. The alkali is always added in excess to the stoichiometric amount in order to maintain high pH of 12 during the crystallization reaction. The dry condition at the grinding step is necessary because in the presence of water,

it forms cement like material called as geopolymer, which immediately sets hard and damages the grinder impeller. The ground material is allowed to settle in the grinder pot for about 20 minutes and is then carefully transferred into a dry silica crucible and immediately kept in the furnace maintained at 700 °C.

3.1.2 Fusion Reaction

The fusion step is very crucial in this synthesis procedure because to a large extent it decides the crystallinity of final zeolite. The good fusion means complete conversion of free silica and alumina (present in the flyash) into a mixture of the sodium silicates and sodium aluminate. When the silica and alumina is completely converted into the sodium silicate and sodium aluminate, the fused mass in the furnace becomes light blue in colour. We have optimized the fusion temperature by carrying out fusion at varying temperature between 400 to 700 °C. It is found that the fusion is very poor upto 600 °C as evidenced by an absence of the light blue colour of the fused mass withdrawn from the furnace. At 700 °C optimal results are obtained. Hence thereafter, we carried out fusion reaction at 700 °C for about 2 hours. After cooling this fused mass to room temperature, it is again ground in order to break the lumps, which are formed during the fusion.

3.1.3 Nucleation of Aluminosilicate

The well ground fused mass is then mixed with distilled water in the ratio of 1:4 and kept for agitation for about 8 hours at room temperature. The small amount standard zeolite seed is also added to this, in order to facilitate

the nucleation of aluminosilicates zeolite. At the end of the agitation, the green colour slurry of the fused mass turns to white.

3.1.4 Alumina Makeup by Sodium Aluminate

Before this slurry is kept for the crystallization reaction, the alumina makeup is needed for maintaining silica alumina ratio at 1.0-1.5. This is done by adding sodium aluminate to it. First we used commercially available sodium aluminate powder, which is found to give amorphous zeolite, which had low cation exchange capacity and specific surface area. This might be due to the fact that the powder sodium aluminate is not completely soluble in water medium. So, we prepared sodium aluminate solution by refluxing the mixture of $\text{Al}(\text{OH})_3$ (60 g), NaOH pellets (65 g) and distilled water 250 ml at 80 °C for 6 hours. The reflux mass is filtered and the filtrate is a light yellow solution with approximately 15 % sodium aluminate concentration. The crystallinity and the cation exchange capacity of the resulting zeolite are found to be improved when the sodium aluminate is used in the solution form.

3.1.5 Crystallization Reaction of Flyash Zeolite

After the alumina makeup, the agitated slurry is kept for the crystallization reaction at 105 °C and autogenous hydrothermal pressure (1.3 atm). The crystallization reaction involves the incorporation silica and alumina into the nuclei of the aluminosilicate in the soluble form and subsequently precipitation of this aluminosilicates zeolite. The crystallization temperature of

105 °C is found to be sufficient for the building of hydrothermal pressure of 1.3 atm. The crystallinity of the resulting zeolite(Z-A-5) is found to be decreased when the reaction is carried out below 95 °C. This is because, the necessary hydrothermal pressure of 1.1 atm. needed for the incorporation of silica and alumina into the zeolite matrix and precipitation of zeolite is not created at this temperature. The crystallization reaction carried out at 105 °C is found to give the best crystallinity. The incorporation of silica into the zeolite matrix is the rate-controlling step. The reaction time for A-type zeolite (3 hours) is less than Y-type zeolite (12 hours) because silica content of the former is less than that of the latter. The commercial process for zeolite-A synthesis uses the sodium silicate and sodium aluminate as the raw material for silica and alumina source. This commercial process for the zeolite-A synthesis needs about 5 hours whereas the flyash zeolite synthesis procedure needs only 3 hours. This is because, the flyash is known to contain some electrically charged molecules which enhances the rate of the crystallization. After the crystallization is over, the reaction mass is filtered and the mother liquor is collected as filtrate. The aluminosilicate zeolite is washed thoroughly with distilled water to remove all alkalinity. Then it is dried in an oven at 100 °C.

3.2 Synthesis of Flyash Zeolite with Varying Si/Al Content

The following two approaches can change the silica content in the aluminosilicate zeolite

1. By direct addition of sodium aluminate into the agitated slurry of the fused mass before it is kept for the

crystallization, keeping the time of the crystallization reaction constant.

2. By varying the time of the crystallization reaction but keeping initial silica – alumina ratio in the fused mass constant.

We have synthesized a series of flyash zeolite with varying silica-alumina content. This is done by the addition of sodium aluminate solution into the well-agitated slurry of the fused mass keeping the time of the crystallization constant at 3 hours. Table 3.1 shows the chemical formulation and process condition for the synthesis of the flyash zeolite with varying silica–alumina content. In all experiment, we have started with 20 g of air-dried flyash and 25 g of NaOH. The fusion temperature was initially kept at 600 °C and a change in to 700 °C produced little change in crystallinity (discussed later in the Table 3.3) .In some of the experiment the makeup sodium aluminate was the commercial material in the form of powder and in some, it was in the form of solution. We noticed (as discussed later in the Table 3.3) that the solution form of the sodium aluminate gave higher crystallinity and cation exchangeability. This is because the powder sodium aluminate does not completely go into the solution and undissolved material goes under polymerization to give amorphous geopolymer.

3.3 Structural Characterization of Flyash Zeolites using XRD

In order to carry out the structural characterization of these flyash zeoliteS, we have recorded their X-Ray Diffraction (XRD) patterns. During all XRD analysis, the X-Ray wavelength is kept constant at 1.5406 °A and the

relative intensity of the diffraction is recorded as the function of 2θ . In general absence of sharp peaks reveals the presence of amorphous region in the zeolite and except for Z-A-5 given in Table 3.2, all other zeolite are found to have sharp peaks. We have used the XRD analysis of the standard Na-aluminosilicate zeolite reported in the JCPDS file⁴⁷ for the structural characterization of our flyash zeolite. This file has a record of about two hundred zeolite and we compared our XRD result with record No. 38 to 238 for sodium aluminosilicate zeolite. For this, we have first chosen the first five strong XRD peaks of the flyash zeolite and reported their relative intensities versus 2θ in the Table 3.2. Then we searched the standard sodium aluminosilicate zeolite from the JCPDS file whose first five strong XRD peaks gets matched approximately with the five strong XRD peaks of our flyash zeolite. The same table shows the comparative XRD values of the flyash zeolite and its most closely matching standard zeolite chosen from JCPDS files. The percentage relative crystallinity of flyash zeolite compared to its most closely matching standard zeolite is found by taking ratio of the sum of the relative intensities (all five strong XRD peaks) of the flyash zeolite to the sum of the relative intensities (all five strong XRD peaks) of standard zeolite. It is found that the percent relative crystallinity of the flyash zeolite compared to standard zeolite is nearly 100 percent as shown in Table 3.3. The structural properties of standard zeolite with reference to molecular structure, geometry of structure, and molecular weight is reported in the JCPDS file. We have carried out the structural characterization of our flyash zeolite by assuming that flyash zeolite is having nearly the same structural framework as the standard zeolite reported in the JCPDS file. Hence we have directly taken

these molecular data from standard JCPDS file and reported this information in Table 3.3.

3.4 Surface Area Analysis of Flyash Zeolites

We have carried out the specific surface area analysis of flyash zeolite using BET Surface Area Analyzer (Model No. SA-3100, Coulter Company, England).

The specific surface area of our flyash zeolite is found to vary between 230 m²/g (zeolite Z-A-3) to 325 m²/g (zeolite Z-A-1). It is found that, the specific surface area of our zeolite gets highly improved when alumina makeup is done by sodium aluminate in the solution form.

3.5 Particle Size Distribution of Flyash Zeolites

We have also carried out the particle size analysis of all flyash zeolites and the standard zeolites procured from Japan. This analysis is carried out using Laser Particle Size Analyser (Fritsch GMBH, Germany).

Table 3.4 gives the particle size distribution of flyash zeolite and the standard zeolites. This table gives the record of percentage of particles with particle size less than 1 μm , 4 μm , 7 μm , and 10 μm . The average particle size range is that range in which 50 to 80 % of particle lie. Except zeolite Z-R-6, whose particle size is approximately same as standard zeolite-A (Wako Japan), on an average the particle size of the rest of the flyash zeolite is found to be varying between the 3 to 5 μm . This particle size distribution range of our flyash zeolite (3–5 μm) is found to be in good approximation with standard zeolite-A (3.6 – 5.2 μm) procured from Degussa, Japan.

3.6 Structural Analysis through Scanning Electron Microscopy

In order to study the geometry of structure, we have carried out the Scanning Electron Microscopy (SEM) test of our flyash zeolite (Z-A-4) as well as standard zeolites (wako, Japan and Degussa, Japan) using the Jeol-840-A Scanning Electron Microscope. Figure 3.1 shows the SEM photograph of these zeolite that reveals that, the structural framework is highly crystalline with nearly cubic geometry.

3.7 Moisture Content and Water of Hydration of Flyash Zeolite

The water content of sodium aluminosilicate zeolite exists in loosely bound moisture as well as chemically bound Water of Hydration. The former can be removed by heating at 110 °C for two hours while the water of hydration can be removed by heating zeolite at about 800 °C for 2 hours. At this point zeolite loses its crystallinity and its structure is also breaks down. We have determined the moisture content as well as the water of hydration of our zeolite using the procedure discussed in section 2.3.5. The Table 3.5 summarizes the data of the moisture content and the water of hydration of flyash zeolite and standard zeolite. The moisture content of our zeolite is found to vary between 4.5 to 6.0 % while later varies between (16.5 to 20 %). The water of hydration is found to be very close to that of standard zeolites (17.3 to 19.0 %) and this table shows that this does not very much depend upon Si/Al ratio.

3.8 Cation Exchange Capacity Flyash Zeolite

The aluminosilicates zeolites have excellent cation exchange capacity. We have determined the cation exchangeability of our flyash zeolite using the standard procedure discussed in the section 2.3.6. Table 3.6 summarizes the results for our zeolite and standard zeolites. The cation exchangeability is expressed in meq. per gram of oven dry mass of zeolite. The table also gives the cation exchange capacity of zeolite after regeneration. The cation exchangeability of our zeolites is found to increase sharply with the decrease in Si/Al ratio. This is because in the aluminosilicate zeolite, the exchanging cation Na^+ chemically bound to Al^{3+} atom. This negative charge cation site in our zeolite is increase with the aluminum atom in the zeolite matrix. The results reveal that the cation exchangeability of regenerated zeolite is about 10 % less than fresh zeolite. However the cation exchange capacity of zeolite Z-A-6 (83.8 % crystalline) and Z-R-6 (90.5 % crystalline) has been reduced drastically to about 50 % on the regeneration. This is because these zeolites have relatively amorphous structure.

3.9 Nitration of Flyash Zeolites

Nitration of flyash zeolites have been carried out by the gas phase nitration reaction at 225 °C described in the section 2.4. The Table 3.7 gives the details of experimental conditions and it is observed that for a single run nearly 18 hours of reaction time is needed for the complete consumption of 1000 ml of NO_x gas by the 15 gram of air-dried zeolites. It is found that during the reaction, water is adhered to the wall of the glass reactor. This water is removed from the reactor before it is filled with NO_x to start the next run. We

have this way carried out the nitration in 15 installments (1000 CC of NO_x per run) till the zeolite became saturated and consumption of NO_x stops. We found that approximately 15 such runs are needed to reach this saturation point.

We have presented the photographs of the modified zeolites in figure 3.2, which shows the colour change of the blank zeolite (A-4) from cream white (figure 3.2 a) to pale yellow upon nitration (figure 3.2 b). The amination of this nitrated zeolite gives the further change in colour (cream yellow) as shown in figure 3.2 c.

3.10 Identification of Functional Groups through the FTIR Analysis

In figure 3.3 we have presented the FTIR spectra of our blank zeolite and functionalised flyash zeolite. On comparing the IR spectra of the blank zeolite A-4 with that for the nitrated and the aminated flyash zeolite, a characteristic sharp peaks of NO_2 group in spectra (b) is seen at 700 and 1400 cm^{-1} . The aminated zeolite on the other hand in spectra (c) shows the strong absorption $-\text{NH}_2$ peak at 3500 cm^{-1} with the simultaneous disappearance of peaks at 700 and 1400 cm^{-1} belonging to NO_2 . Figure 3.4 shows the IR spectra of dichloroethane-modified zeolite (spectra-a) and trimethylamine quarterized zeolite (spectra-b). Due to overlapping, these spectra do not show a separate peak for chloride group.

3.11 Elemental Analysis of Modified Flyash Zeolite In order to find the number of equivalents of nitrogen attached per repeat unit of zeolite matrix, we have carried out the elemental analysis of the nitrated as well as aminated zeolites using elemental analyser. This elemental analysis shows that approximately 3.85 % of elemental nitrogen is present per gram of oven dried (nitrated as well as aminated) flyash zeolite. The number of equivalents of nitrogen attached per repeat unit of zeolite (defined as that part of the aluminosilicate zeolite matrix which contains one charge compensating exchangeable sodium ion) matrix is found out by following relation.

$$\text{Number of equivalents of nitrogen} = \frac{M \times (\%N)}{14}$$

attached per repeat unit of zeolite

Where,

M= Molecular weight of one repeat unit of zeolite matrix.

This is calculated for each flyash zeolite and summarized in the Table 3.7. It is found that except for few zeolites (R-3, R-4, R-5, and A-2), the number of equivalents of nitrogen attached to the repeat unit increases with the increases in the amount of silica in the zeolite matrix as seen in Table 3.7.

3.12 Electron Spectroscopy for Chemical analysis (ESCA)

In order to see whether (-NO₂) is just chemisorbed or it is attached to the Si atom of zeolite matrix covalently, we carried out the Electron Spectroscopy for Chemical analysis (ESCA) for the blank and nitrated samples of silica gel and quartz sand. The silica gel and the quartz sand have

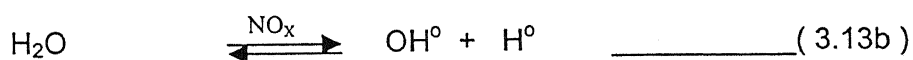
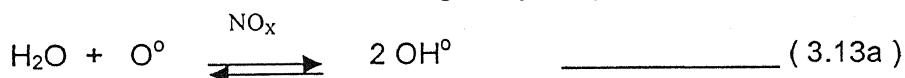
Si 2p binding energy peaks in the range of 105 – 145 (figure 3.5) and 150 – 190 eV (figure 3.6). The Si 2p peaks for unmodified quartz sand lies at 112 eV (figure 3.5) and 163 eV (figure 3.6), which on nitration shifts to 112 eV (figure 3.5) and 162.5 eV (figure 3.6) respectively while N 1s has a peak at 417 eV. As oppose to this the amorphous silica gel has Si 2p peak at 113 eV (figure 3.5) and 170 eV (figure 3.6), which on nitration shifts to 115.5 (figure 3.5) and 168 eV (figure 3.6) respectively while the N 1s peak occurs at 418 eV (figure 3.7). The difference in the Si 2p binding energy peak positions between quartz sand and silica gel are due to the difference in the crystallinty and for given material, modification by NO_x produces a slight shift in binding energy, this way confirming the formation of Si-N bond.

3.13 Mechanism of Nitration Reaction of Flyash Zeolite

The reaction involving NO_x has been well studied in the problems of pollution phenomena arising due to NO_x in atmosphere ^{49,50}. The reaction is assumed to be triggered by nitrogen & the NO₂ and in their presence oxygen radical (O°) is formed as follows.

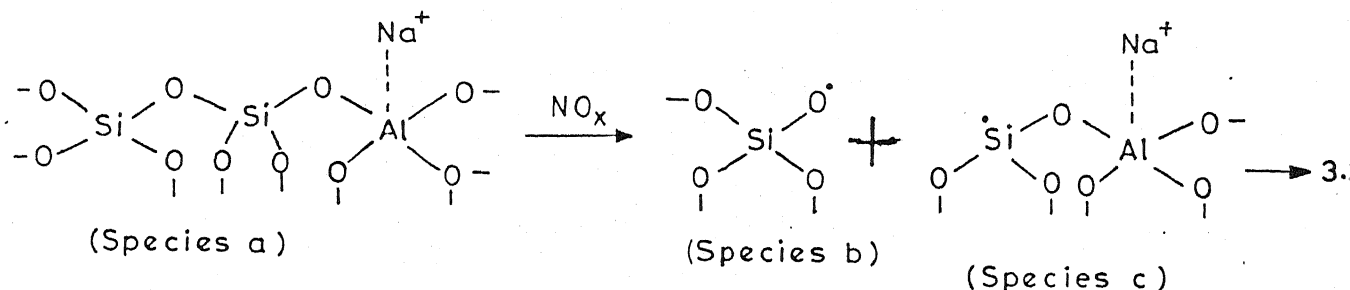


This oxygen radical reacts with moisture to give hydroxyl radicals as follows.

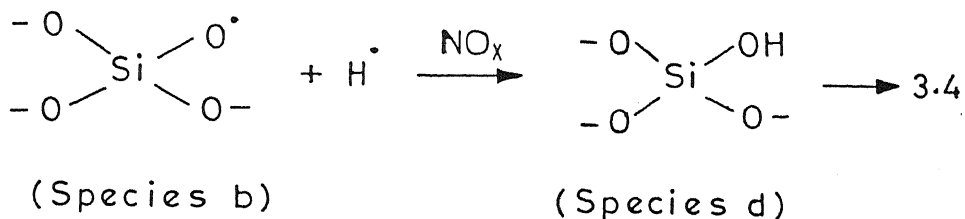


This hydrogen radical is active species, which are assumed to give reactions involving NO_x. Our aluminosilicate zeolite consists of Si and Al tetrahedron

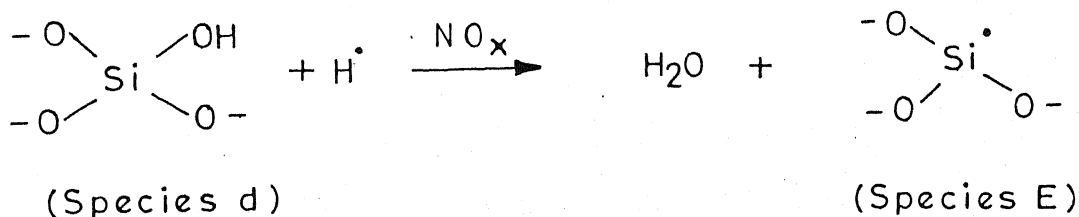
connected by common oxygen sharing (species a). During the gas phase nitration, the Si-O bond is broken in the presence of NO_x as follows.



The Al-O bond does not break during the nitration is confirmed from the fact that the cation exchange capacity of our zeolite remains unchanged even after the nitration and amination. This oxygen radical (species b) is attached to the $(\text{SiO}_4)^-$ tetrahedral and reacts with hydrogen radical (H^\bullet) to give the hydroxyl group (species d) as shown below.

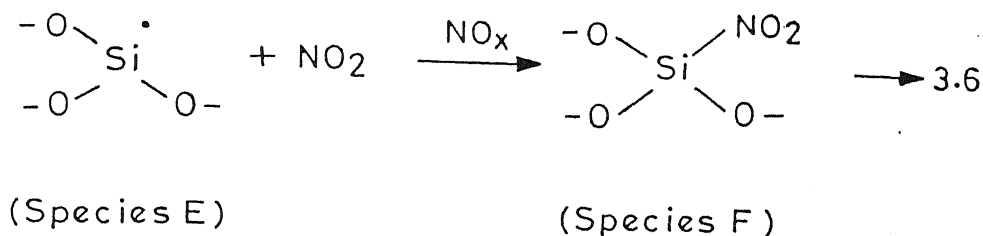


The presence of hydroxyl group in the nitrated zeolite is confirmed by the XRD analysis discussed later in this chapter. The active H^\bullet radical again reacts with this hydroxyl group, which creates an active site on the silicon (Si) atom (species e) as shown below.



→ 3.5

In addition to this, water of hydration is also released and found to adhere to the wall of the glass reactor. Every time, before the start of new run of nitration this water reaction is removed in order to facilitate the reaction 3.5. The active site on the silicon (Si) atom of the zeolite matrix now easily reacts with NO_2 (which is a stable radical) present in NO_x to give $-\text{NO}_2$ group attached to the Si atom of zeolite matrix as follows.



This $-\text{NO}_2$ group of nitrated zeolite is converted into the exchangeable $-\text{NH}_2$ group by amination.

3.14 Crystallographic study of Modified Zeolite

We have recorded the XRD pattern of the nitrated flyash zeolite in order to study the crystallographic changes in it due to nitration. In figure 3.8, we have presented the XRD pattern of both modified as well as unmodified zeolite. It is observed that their XRD patterns are completely altered upon nitration. From the JCPDS cards, we chose the most closely matching standard sodium aluminosilicate zeolite (File No. 24-1047) adopting the same procedure discussed earlier in the section 3.3. The Table 3.8 gives the d-spacing and relative intensity values of XRD analysis for the zeolite A-4, and nitrated zeolite A-4 and their most closely matching standard zeolite. The

molecular structure of this nitrated zeolite is $\text{Na Al}_2 (\text{AlSi}_3\text{O}_{10}) (\text{OH})_2$ with the same Si/Al ratio of 1.0 as that of unmodified zeolite (A-4). The presence of the hydroxyl group on the repeat unit supports the postulated mechanism. This nitrated zeolite is found to have 100 percent crystallinity (with respect to standard zeolite, JCPDS File No. 24 -1047) and has a monoclinic crystal structure. This change in the crystal structure of the zeolite upon nitration confirms that, Si-O bond must have broken.

3.15 Anion Exchange Capacity of Modified Zeolite

The anion exchange capacity of the aminated zeolite arises due to the exchangeable amine ($-\text{NH}_3^+\text{Cl}^-$) group and is determined by the standard amination procedure discussed in the section 2.8. The Table 3.9 gives the anion exchange capacity of the aminated zeolite in meq. per gram of the oven-dry mass of the aminated zeolites. It is found that, the anion exchangeability of our zeolite varies between 1.65 to 2.4 meq. /g and increases with the increase in the silica content of the zeolite. This is because the Si atom of the zeolite gives the Si-N bond whereas Al is responsible for the cation exchangeability and does not react with the NO_x .

3.16 Anion Exchangeability of Quarternized Flyash Zeolites

In order to see whether the aminated zeolite responds to organic reactions, we reacted it with dichloroethane. The chloroethylated zeolite is quarternized with trimethylamine by adopting the procedure given in the section 2.6. We have determined the anion exchangeability of this modified zeolite using the ASTM procedure and Table 3.9 gives the anion exchange

capacity of this quarternized zeolite. It is observed that the anion exchangeability is doubled indicating that two dichloroethane molecules reacts with every amine group in the zeolite. The anion exchangeability of regenerated quaternized zeolite is found to be approximately 70 percent of fresh zeolite. This is because of the equilibrium formation between exchanging groups. We have also found out that, the cation exchange capacity of these zeolites does not change due to these modifications.

3.17 Characterization of Mesoporous Silica

We have synthesized three set of mesoporous silica, two from TEOS with varying surfactant amount and one from the flyash mother liquor. In order to find the crystallinity, we have recorded their XRD patterns. It is found that these mesoporous silica have amorphous structure as evidenced by the absence of sharp peaks. We have determined the Specific surface area (m^2/g) and Pore volume (cc/g) of these mesoporous silica using the same machine discussed in the section 2.3.2. The surface area of the mesoporous silica is found to be in the range of 833–841 m^2/g . pore volume of these, found to vary between 0.5-0.53 cc/g . It is found that surface area of mesoporous silica prepared from TEOS decreases whereas pore volume increases with increase in surfactant amount. The surface area of flyash mesoporous silica is found to reduce to a low value of 398 m^2/g . This can be improved by manipulating the process conditions & formulations. The average particle size range of mesoporous silica is found to be (19.6–31.0 μm) for TEOS mesoporous silica and (14.0–25.5 μm) for flyash mesoporous silica. These results are summarized in the Table 3.10.

3.18 Modification of Mesoporous Silica using NO_x

We have modified one set of these mesoporous silica using NO_x and subsequently aminated it following the same procedure of that for flyash zeolite. It is found that approximately 2400 CC of NO_x is consumed per gram of air-dried mesoporous silica. We have presented the photographs of the modified mesoporous silica in figure 3.9, which shows the colour change of blank mesoporous silica from pale white (figure 3.9 a) to cream white upon nitration (figure 3.9 b). The amination of this nitrated mesoporous silica gives the further change in colour (cream yellow) as shown in figure 3.9 c.

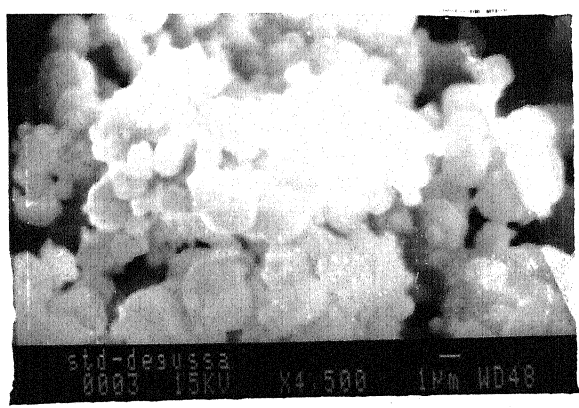
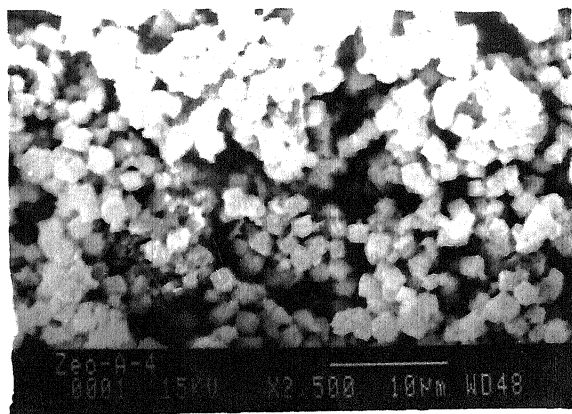
3.19 Analysis of Functional Groups through FTIR analysis

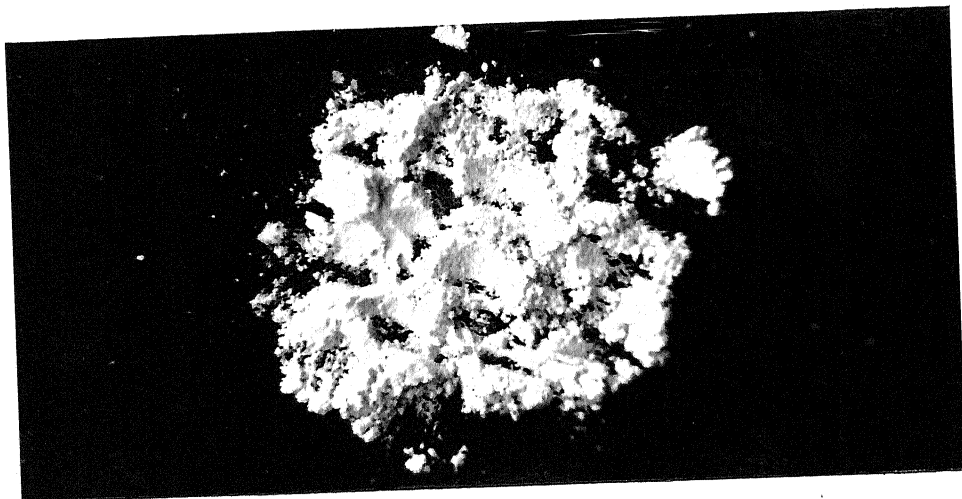
Figure 3.10 shows the FTIR spectra of blank, nitrated and aminated mesoporous silica. It is seen that the characteristic sharp peak of $-\text{NO}_2$ appears at 1400 cm^{-1} (curve b) in nitrated mesoporous silica. The strong $-\text{NH}_2$ peak is seen at 3500 cm^{-1} (curve c) with the simultaneous disappearance of peaks at 1400 cm^{-1} belonging to Nitrate group.

3.20 Anion Exchangeability of Modified Mesoporous Silica

We have determined the anion exchange capacity of this modified mesoporous silica using the standard ASTM procedure discussed in section 2.8. It is found that anion exchange capacity of this mesoporous silica is 2.3

meq. / g which on the modification with dichloroethane and trimethylamine increases to 2.6 meq./g.

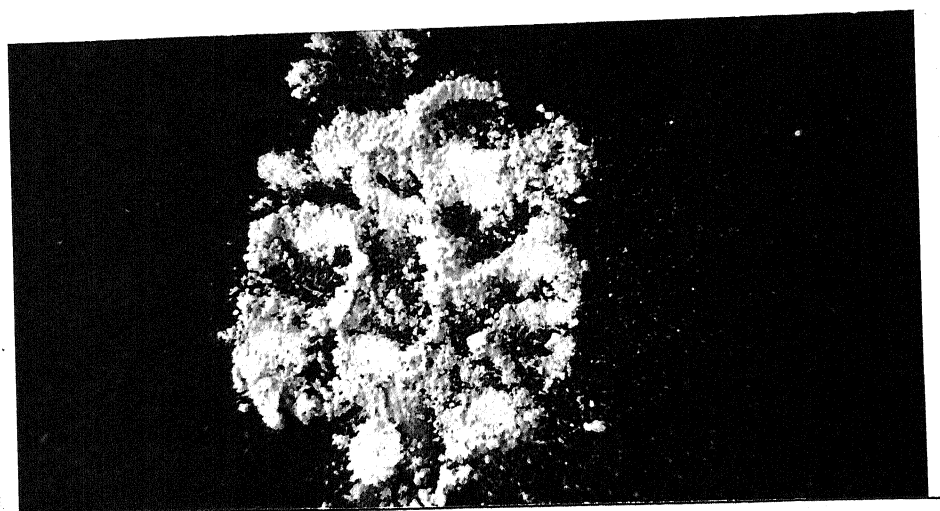




(a)



(b)



(c)

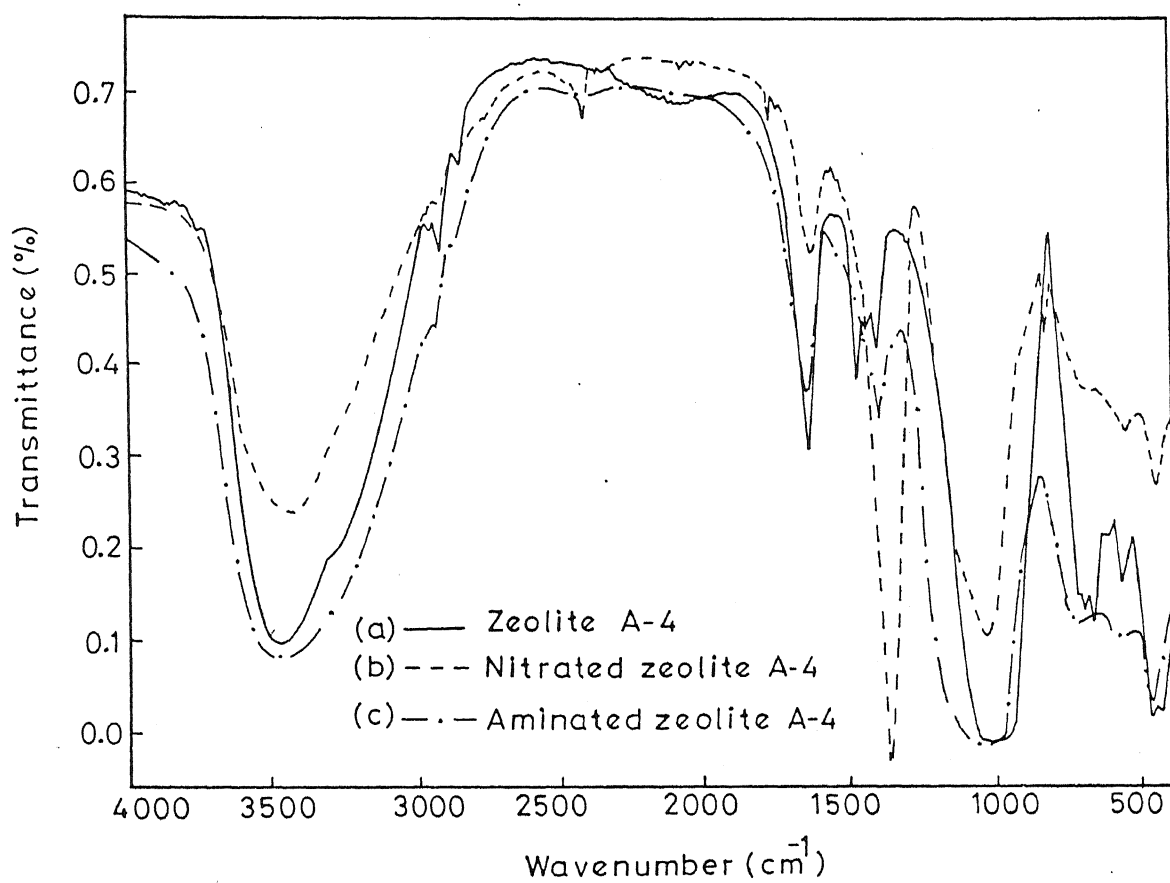


Figure 3.3: FTIR spectra of (a) Blank (b) Nitrated and (c) Aminated flyash zeolite.

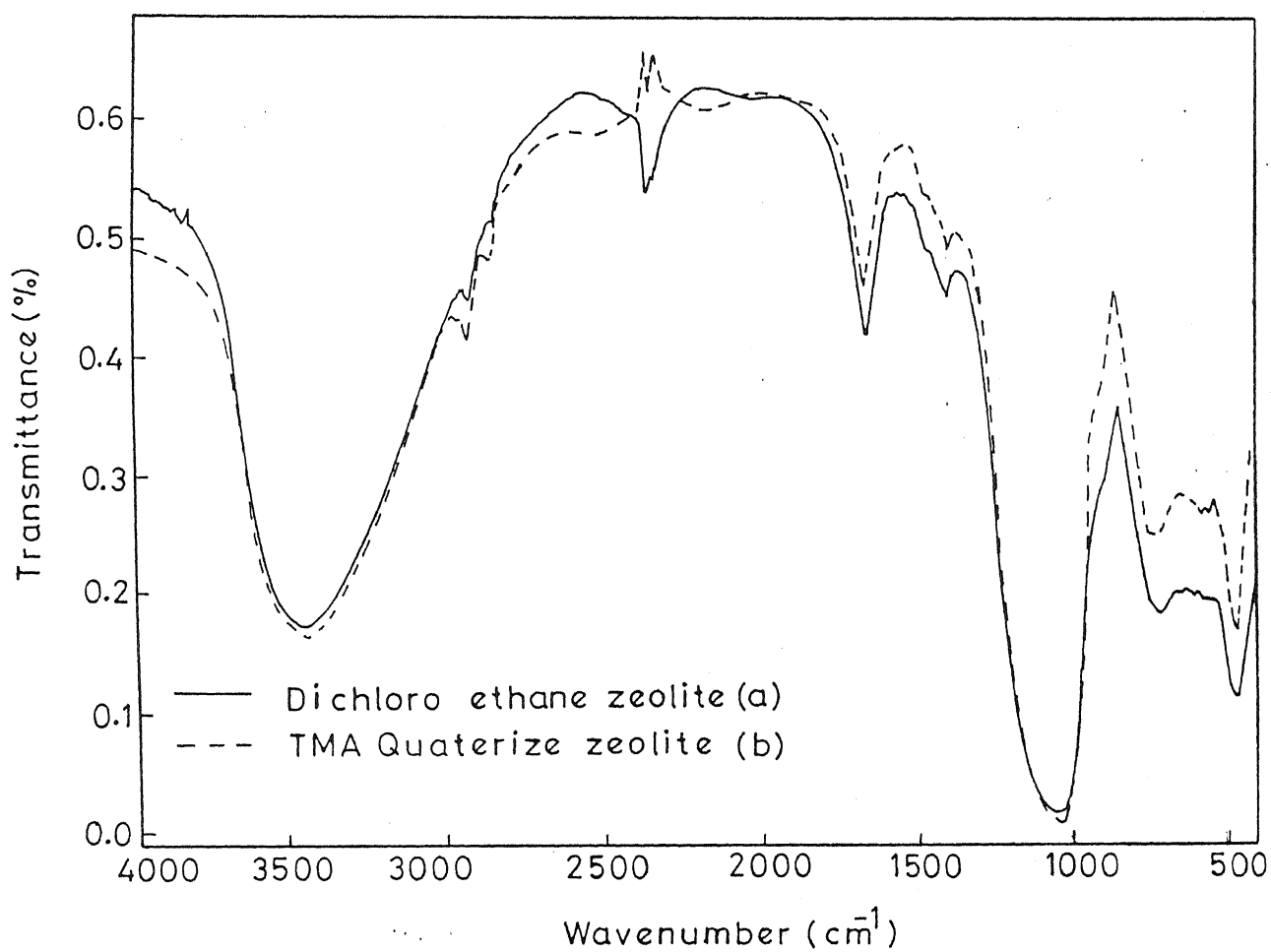


Figure 3.4: FTIR spectra of (a) Dichloroethane modified (b) Trimethylamine quarternized flyash zeolite.

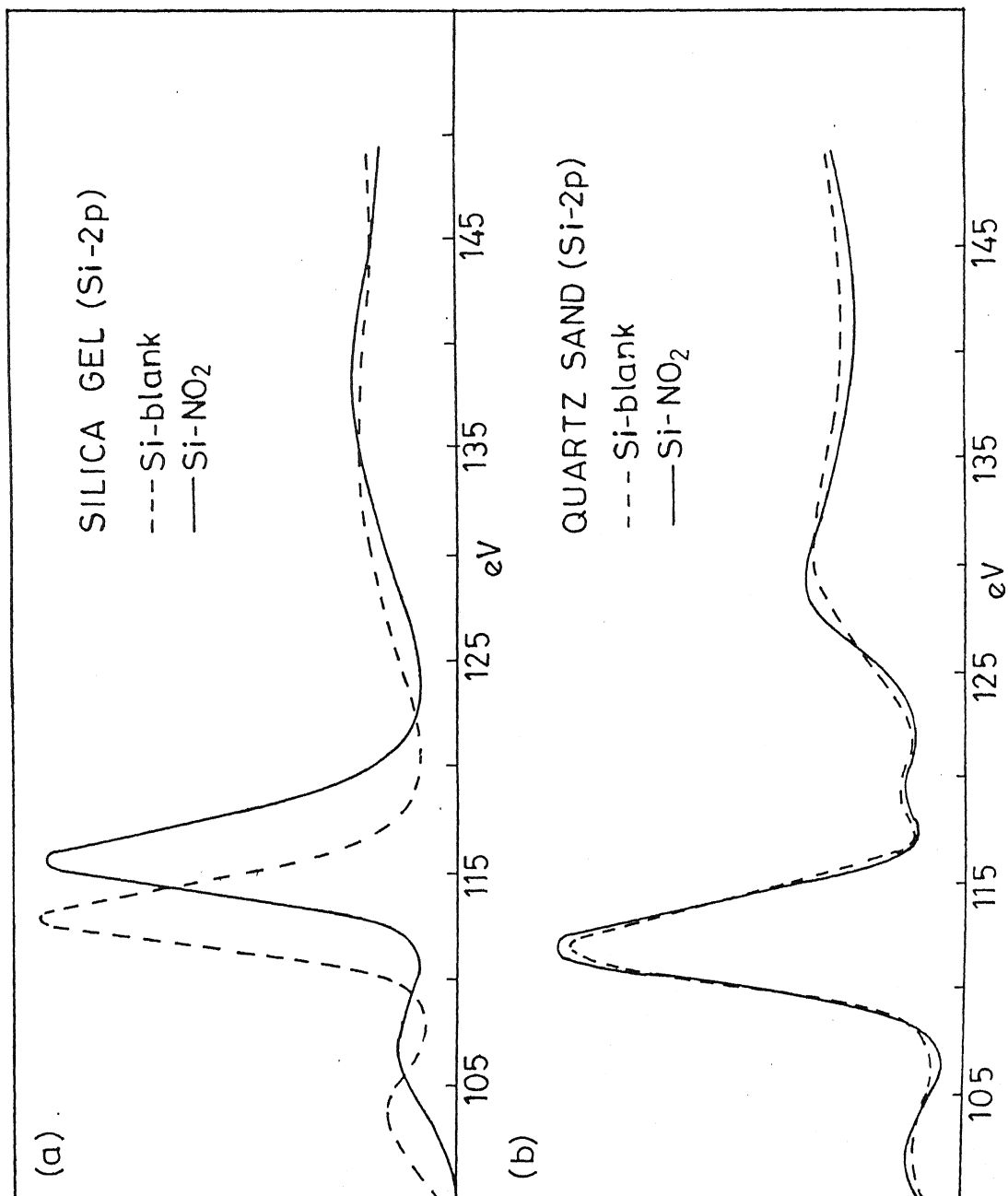


Figure 3.5: ESCA spectra of Si 2p binding energy for the blank and modified

(a) Silica gel and (b) Quartz sand in the 105-145 eV range

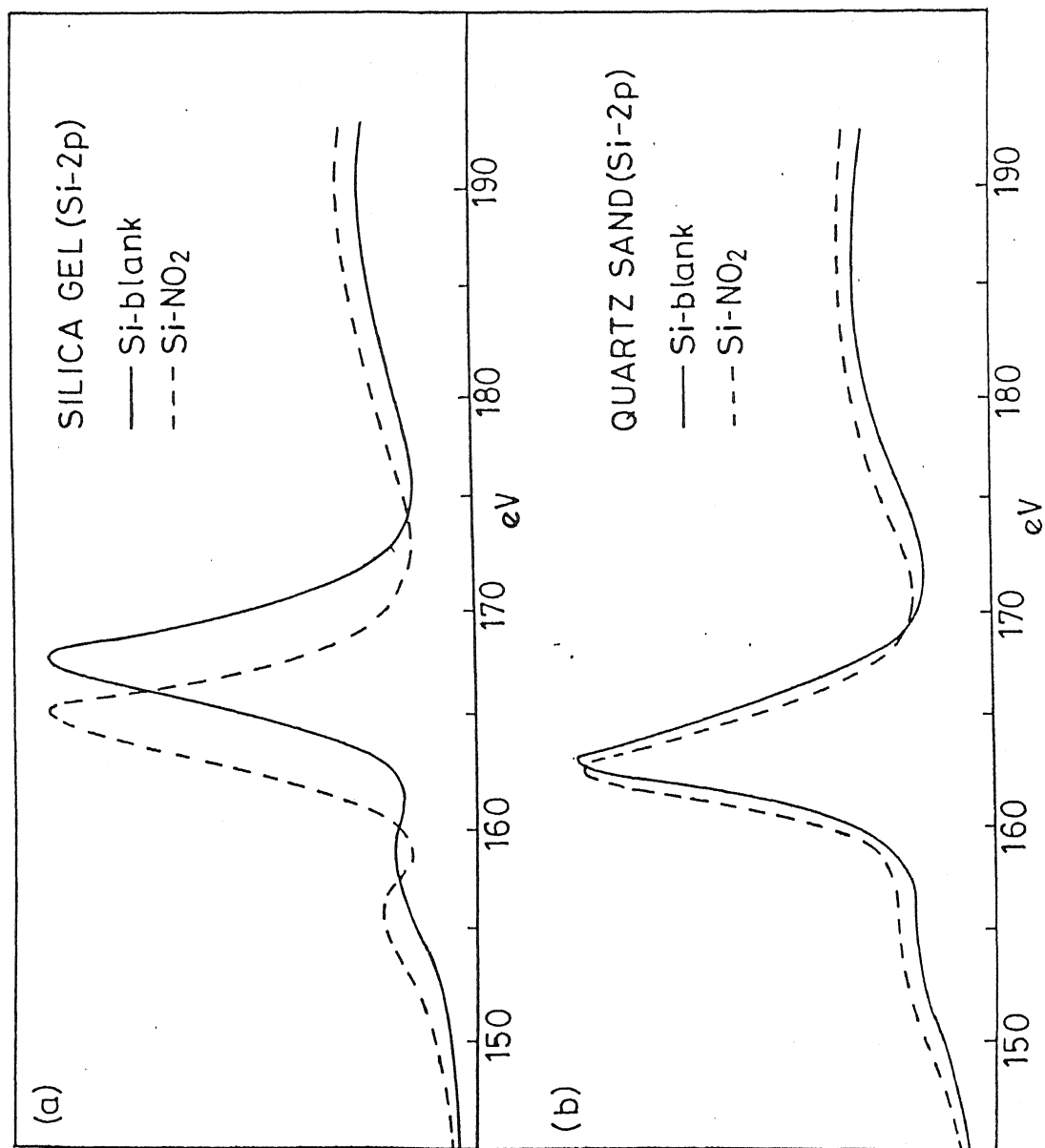


Figure 3.6: ESCA spectra of Si 2p binding energy for the blank and modified

(b) Silica gel and (b) Quartz sand in the 150-190 eV range

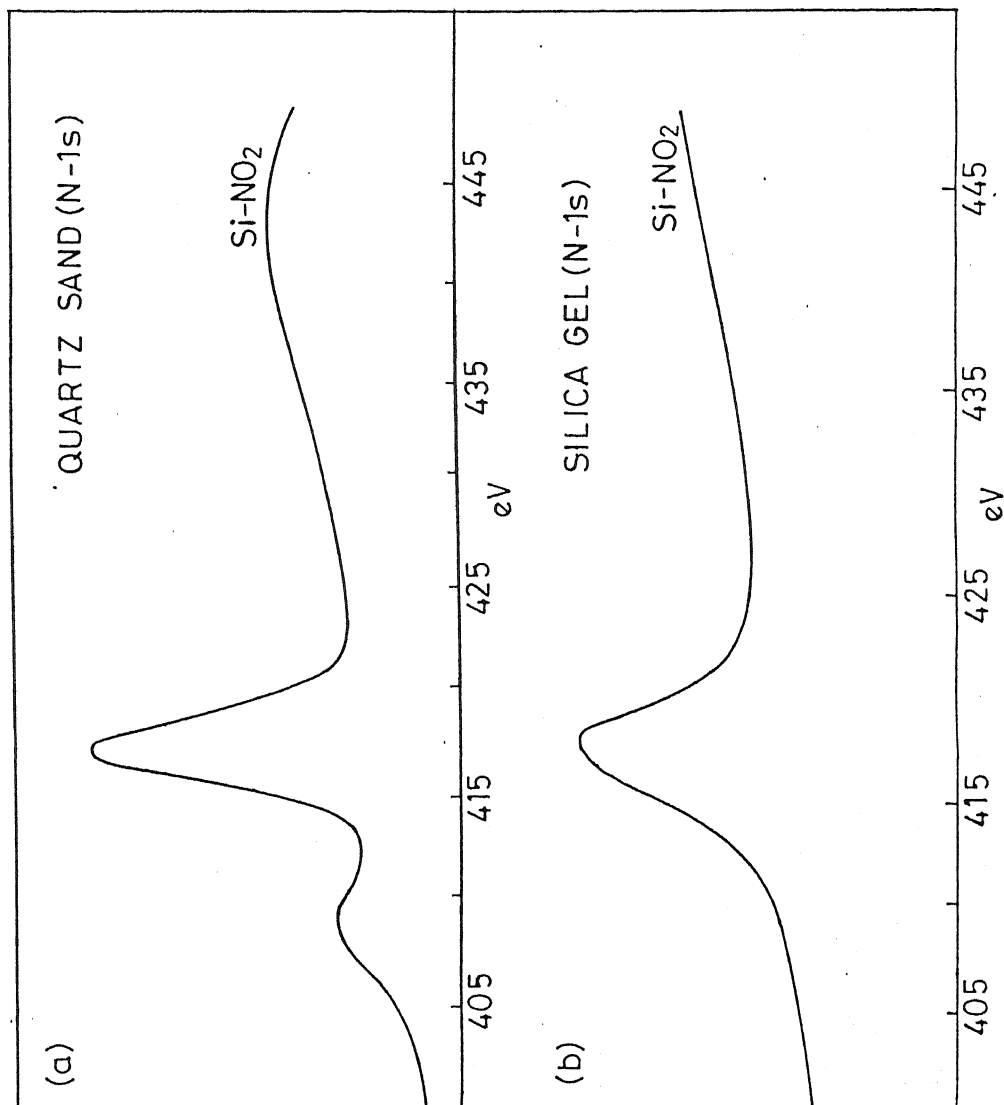


Figure 3.7: ESCA spectra of N 1s binding energy for the modified

(a) Quartz sand and (b) Silica gel

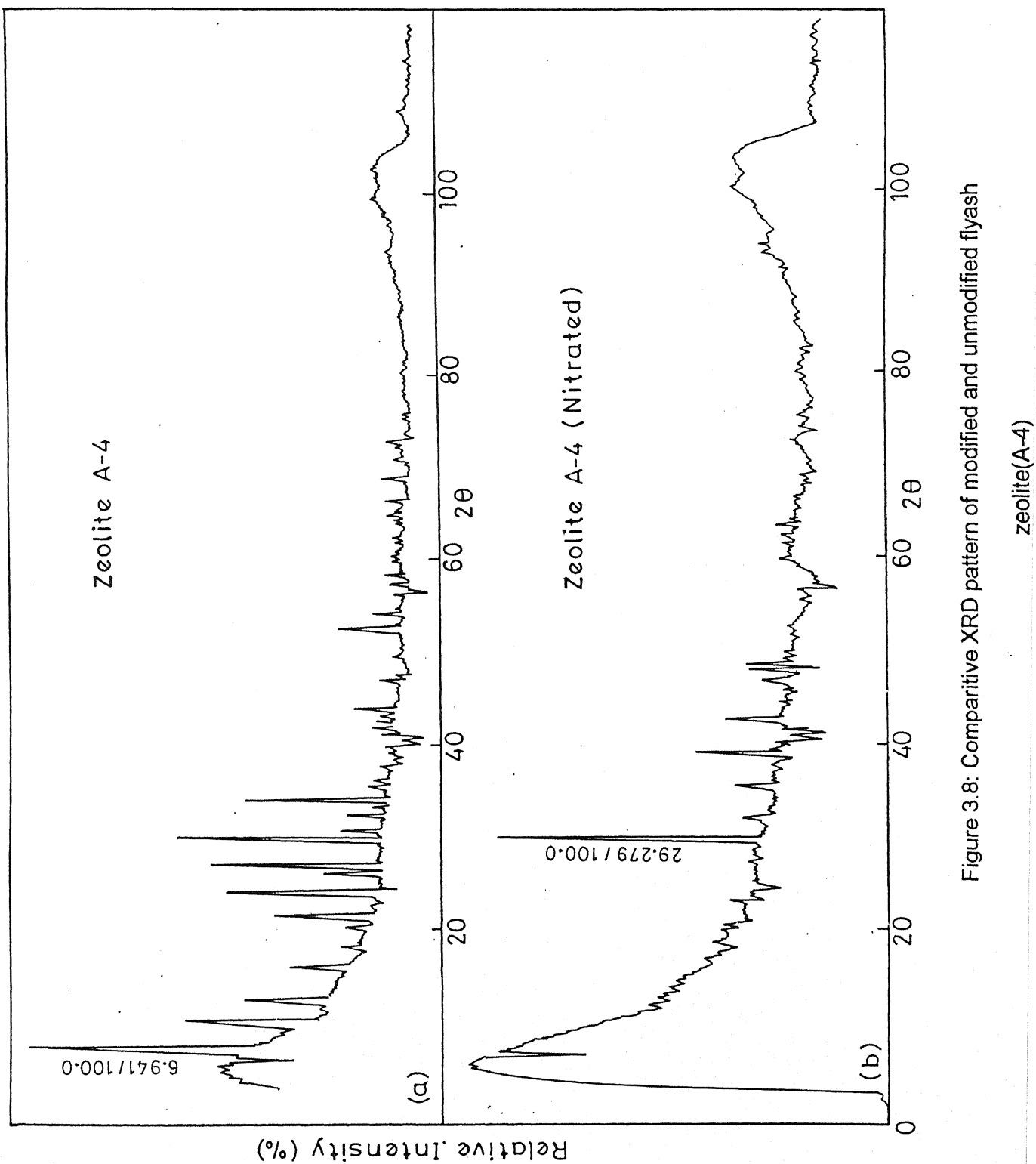
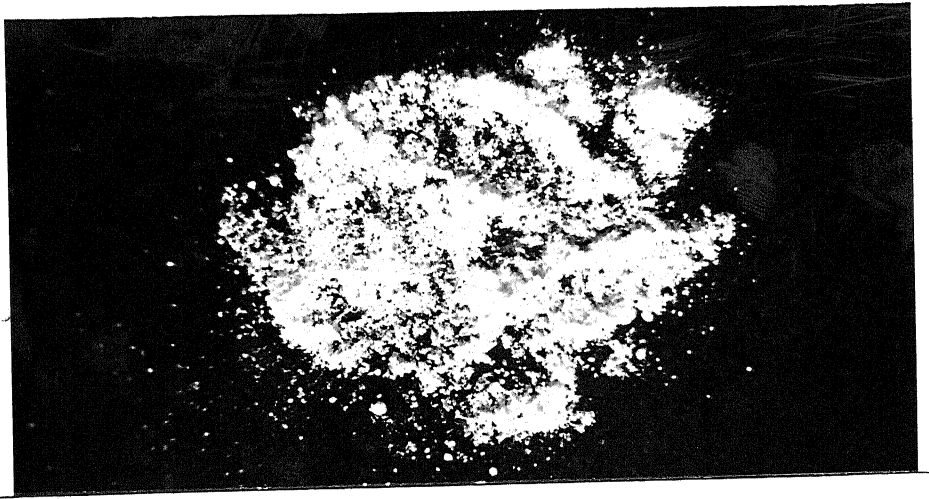
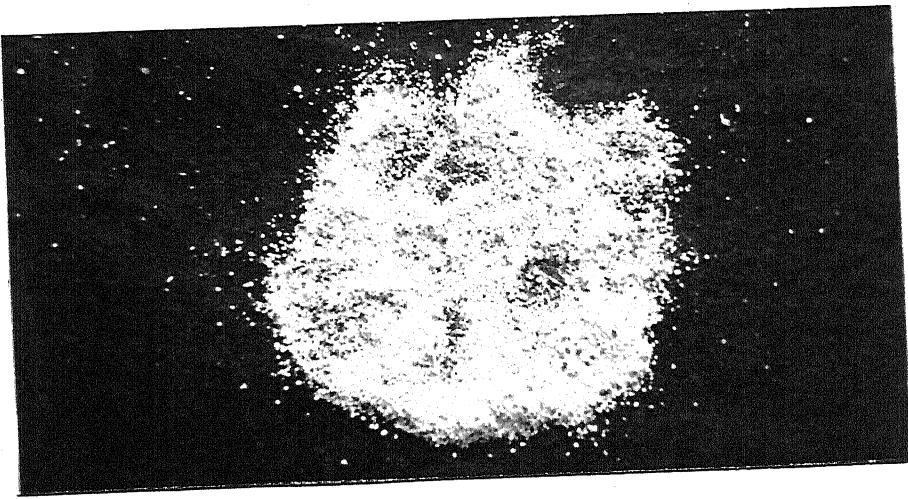


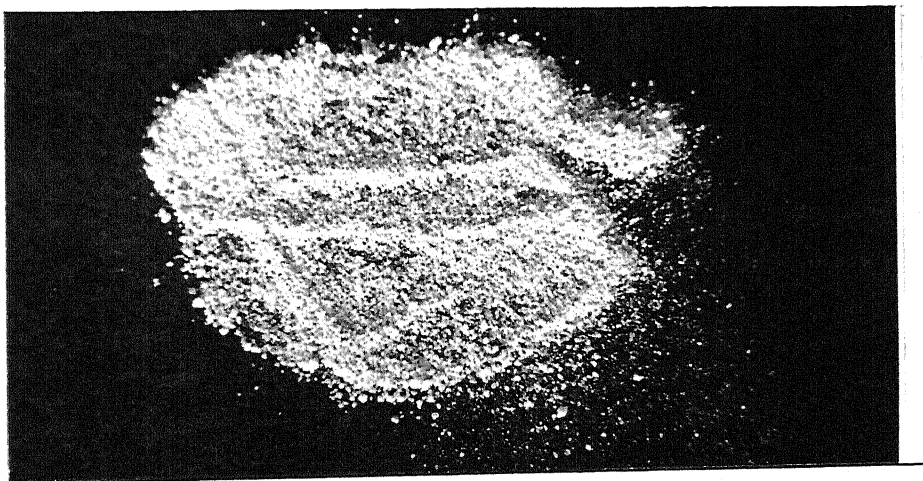
Figure 3.8: Comparative XRD pattern of modified and unmodified flyash



(a)



(b)



(c)

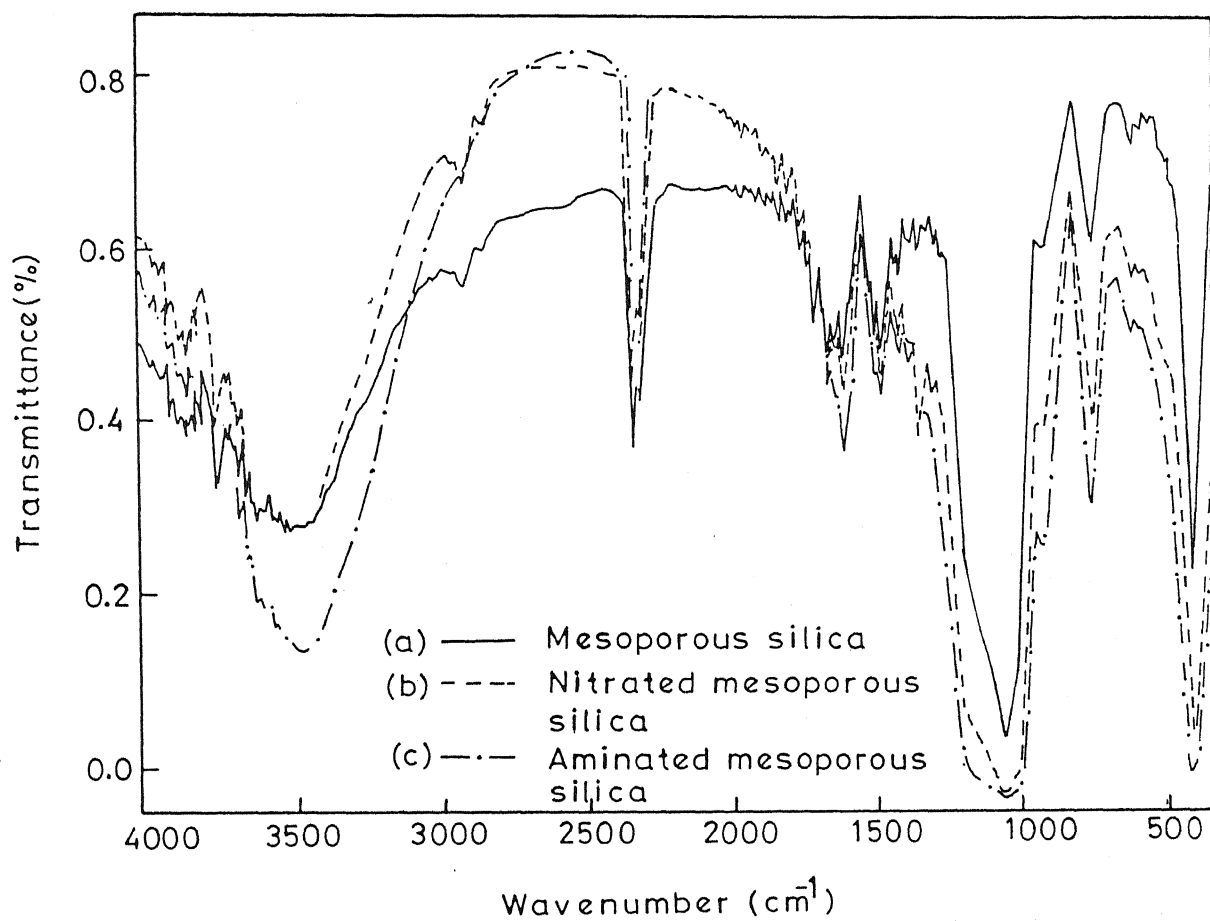


Figure 3.10: FTIR spectra of (a) Blank (b) Nitrated and (c) Aminated mesoporous silica.

Sr. No.	Name of flyash zeolite	Mass of acid treated flyash	Mass of NaOH pellets (grams)	Fusion temp. (°C)	Nucleation time (Hours)	Alumina makeup source		Crystallization reaction temperature (°C)	Reaction time (hours)
						NaAlO ₂ solution (15%)	NaAlO ₂ powder (Grams)		
1	Z-A-1	20 g	25 g	600	8	70.0 ml	-	105	3
2	Z-A-2	20 g	25 g	600	10	65.0 ml	-	105	3
3	Z-A-3	20 g	25 g	600	8	-	04.0 g	105	3
4	Z-A-4	20 g	25 g	600	8	-	14.0 g	105	3
5	Z-A-5	20 g	25 g	650	8	-	06.0 g	95	3
6	Z-A-6	20 g	25 g	650	8	-	08.0 g	105	3
7	Z-R-1	20 g	25 g	700	8	50.0 ml	-	105	3
8	Z-R-2	20 g	25 g	700	8	75.0 ml	-	105	3
9	Z-R-3	20 g	25 g	700	8	0.00ml	0.00 g	105	12
10	Z-R-4	20 g	25 g	700	8	90.0 ml	-	105	3
12	Z-R-5	20 g	25 g	700	8	80.0 ml	-	105	3
13	Z-R-6	20 g	25 g	700	8	60.0 ml	-	105	3

* Flyash has Si/Al ratio of 1.5

Table 3.1: Chemical formulation and process conditions used for synthesis of flyash zeolites with varying silica. alumina content.

Name of zeolite / JCPDS file No.	2 θ ₁ (%RI)	2 θ ₂ (%RI)	2 θ ₃ (%RI)	2 θ ₄ (%RI)	2 θ ₅ (%RI)	Σ RI	Percent crystallinity
Z-A-1	5.92 (100)	9.87 (60.70)	30.86 (42.15)	23.17 (39.00)	15.24 (31.00)	272.85	100.00
File No. 12-246	6.00(100)	9.99 (60.00)	30.35 (40.00)	23.30 (60.00)	15.40 (40.00)	300.00	
Z-A-2	9.86 (100)	6.99 (61.20)	30.90 (53.70)	23.20 (47.50)	23.89 (45.90)	308.10	100.00
File No. 18-1198	9.39 (100)	6.64 (48.00)	30.40 (20.00)	23.30 (48.00)	24.30 (46.00)	308.00	
Z-A-3	5.89 (100)	31.76 (46.00)	26.43 (41.80)	23.10 (36.70)	15.20 (29.40)	254.00	100.00
File No. 11-672	6.10 (100)	32.44 (80.00)	26.38 (20.00)	24.10 (20.00)	16.10 (35.00)	255.00	
Z-A-4	6.94 (100)	29.70 (33.0)	23.69 (72.00)	26.84 (63.11)	33.90 (60.20)	330.30	100.00
File No. 11-590	7.10 (100)	29.87 (55.00)	23.93 (50.00)	27.00 (45.00)	34.10 (20.00)	270.00	
Z-A-6	5.95 (100)	26.52 (42.60)	30.87 (39.30)	23.20 (35.55)	18.20 (32.30)	250.00	83.33
File No. 11-672	6.10 (100)	26.38 (20.00)	32.44 (80.00)	24.10 (20.00)	18.90 (80.00)	300.00	

Table 3.2: Comparative XRD values of flyash zeolite and its most closely matching Na-aluminosilicate zeolite chosen from JCPDS cards

Name of zeolite / JCPDS File No.	2 θ ₁ (%RI)	2 θ ₂ (%RI)	2 θ ₃ (%RI)	2 θ ₄ (%RI)	2 θ ₅ (%RI)	Σ RI	Percent crystallinity
Z-R-1	27.84 (100)	13.74 (98.70)	24.11 (65.40)	34.52 (52.76)	42.68 (47.00)	363.86	100.00
File No. 31-1272	27.4(100)	14.00 (50.00)	24.29 (65.00)	34.54 (40.00)	42.70 (45.00)	300.00	
Z-R-2	6.98 (100)	29.86 (59.60)	9.97 (53.70)	23.90 (51.33)	27.00 (47.50)	288.30	90.50
File No. 11-590	7.10 (100)	29.87 (55.00)	10.10 (70.00)	23.93 (50.00)	27.00 (45.00)	320.00	
Z-R-3	27.90 (100)	12.23 (49.35)	21.44 (48.92)	33.20 (47.20)	45.90 (19.60)	365.00	100.00
File No. 25-779	27.30 (100)	12.30 (80.00)	21.90 (50.00)	33.20 (70.00)	46.20 (20.00)	360.00	
Z-R-4	13.77 (100)	33.00 (80.70)	24.12 (75.43)	21.38 (57.10)	34.53 (55.00)	368.20	100.00
File No. 31-1269	13.75 (100)	33.10 (70.00)	23.87 (80.00)	21.67 (50.00)	34.00 (49.00)	249.00	
Z-R-5	13.76 (100)	33.00 (79.74)	24.12 (74.80)	34.50 (66.89)	42.70 (58.20)	368.20	100.00
File No.31-1269	13.75 (100)	33.10 (70.00)	23.87 (80.00)	34.00 (40.00)	42.00 (35.00)	249.00	

Table 3.2: Comparative XRD values of flyash zeolite and its most closely matching Na-aluminosilicates zeolite chosen from JCPDS cards

Name of zeolite / JCPDS File No.	$2\theta_1$ (%RI)	$2\theta_2$ (%RI)	$2\theta_3$ (%RI)	$2\theta_4$ (%RI)	$2\theta_5$ (%RI)	Σ RI	Percent crystallinity
Z-R-6	13.78 (100)	34.53 (66.40)	42.70 (59.70)	51.75 (34.00)	24.10 (29.80)	270.90	90.50
File No. 10-0057	14.18(100)	34.70 (70.00)	42.10 (50.00)	51.30 (30.00)	23.60 (50.00)	300.00	
Wako (Japan)	6.97 (100)	29.77 (96.10)	23.78 (84.00)	26.92 (60.50)	9.94 (49.70)	390.30	100.00
File No. 14-298	7.20 (100)	30.20 (60.00)	24.20 (60.00)	27.40 (65.00)	10.30 (70.00)	355.00	
Degussa	6.98 (100)	29.80 (90.83)	26.97 (73.66)	23.82 (73.00)	9.96 (51.90)	389.39	100.00
File No. 14-298	7.20 (100)	30.20 (60.00)	27.40 (65.00)	24.30 (60.00)	10.30 (70.00)	355.00	

Table 3.2: Comparative XRD values of flyash zeolite and their most closely matching Na-aluminosilicates zeolite chosen from JCPDS cards

Sr. No.	Name of zeolite	Si/Al ratio	Molecular structure of flyash sodium aluminosilicate zeolite	Geometry of crystal structure	Molecular weight	Percent relative crystallinity
1	Z-A-1	1.24	(Na ₂ O) : (Al ₂ O ₃) : 2.4(SiO ₂) : 6.7 H ₂ O	Cubic	428.84	100
2	Z-A-2	1.50	(Na Al Si ₃ O ₈) : x H ₂ O	Cubic	-	100
3	Z-A-3	2.54	Na ₂ Al ₂ Si _{4.7} O _{13.4} : x H ₂ O	Cubic	-	100
4	Z-A-4	1.00	(Na Al SiO ₄) : 12.27 H ₂ O	Cubic	2191	100
5	Z-A-5	-	-	-	-	Amorphous
6	Z-A-6	1.35	Na ₂ Al ₂ Si _{4.7} O _{13.4} : x H ₂ O	Cubic	-	83.33
7	Z-R-1	1.60	1.06 Na ₂ O : (Al ₂ O ₃) : 1.6 SiO ₂ : 1.6 H ₂ O	Hexagonal	292.6	100
8	Z-R-2	1.00	Na Al SiO ₄ : 12.27 H ₂ O	Cubic	2191	90.5
9	Z-R-3	1.73	Na ₃ Al ₃ Si ₅ O _{16.6} : x H ₂ O	Tetragonal	654.4	82.20
10	Z-R-4	1.00	Na ₁₂ Al ₁₂ Si ₁₂ O ₄₈ : x H ₂ O	Hexagonal	-	100
11	Z-R-5	1.00	Na ₁₂ Al ₁₂ Si ₁₂ O ₄₈ : x H ₂ O	Hexagonal	-	100
12	Z-R-6	1.50	Na ₄ Al ₂ Si ₆ O _{17.2} : H ₂ O	Monolithic	622.5	90.50
13	Wako (Japan)	1.00	Na ₉ (AlO ₂) 9(SiO ₂) : 15.27 H ₂ O	Cubic	2125	100
14	Degussa (Japan)	1.00	Na ₉ (AlO ₂) 9(SiO ₂) : 15.27 H ₂ O	Cubic	2125	100

Table 3.3: Structural characterization of flyash zeolite and standard zeolites using XRD analysis.

Sr.No	Name of zeolite	Percentage of particles less than 1 μm	Percentage of particles less than 4 μm	Percentage of particles less than 7 μm	Percentage of particles less than 10 μm	Average particle size range (μm)
1	Z-A-1	7.57	55.68	81.66	94.49	3.0 - 5.0
2	Z-A-2	14.76	81.28	97.04	99.89	2.0 - 4.0
3	Z-A-3	6.56	71.63	93.98	98.93	2.7 - 4.7
4	Z-A-4	5.53	75.37	97.90	100.00	2.8 - 4.3
5	Z-A-5	5.81	47.76	80.98	97.08	4.8 - 6.9
6	Z-A-6	-	-	-	-	-
7	Z-R-1	7.02	61.86	99.89	99.89	3.3 - 5.3
8	Z-R-2	5.15	74.12	97.75	100.00	2.9 - 4.4
9	Z-R-3	3.74	75.63	98.23	100.00	2.8 - 4.3
10	Z-R-4	6.47	46.03	78.37	96.34	4.4 - 7.2
11	Z-R-5	-	-	-	-	-
12	Z-R-6	4.78	30.45	47.71	65.13	7.4 - 13.0
13	Wako (Japan)	5.69	22.40	32.68	52.32	9.7-13.3
14	Degussa (Japan)	3.82	59.02	94.74	99.87	3.6 - 5.2

Table 3.4: Particle size distribution of flyash zeolites and the standard zeolites.

Sr.No	Name of zeolite	Air-Dry mass W_1 g	Oven- Dry mass (110 °C) W_2 g	Mass after ignition (800 °C) W_3 g	Percent moisture $\frac{(W_1 - W_2) \times 100}{W_1}$	Percent Water of hydration $\frac{(W_2 - W_3) \times 100}{W_2}$
1	Z-A-1	1.0000	0.9415	0.7656	5.85	18.68
2	Z-A-2	1.0000	0.9317	0.7378	6.83	20.81
3	Z-A-3	1.0000	0.9381	0.7855	6.19	16.27
4	Z-A-4	1.0000	0.9524	0.7867	4.76	17.40
5	Z-A-5	1.0000	0.9167	0.7494	8.33	18.25
6	Z-A-6	1.0000	0.9514	0.7599	4.86	20.12
7	Z-R-1	1.0000	0.9427	0.7576	5.73	19.63
8	Z-R-2	1.0000	0.9391	0.7542	6.09	19.69
9	Z-R-3	1.0000	0.9402	0.7394	5.98	21.36
10	Z-R-4	1.0000	0.9528	0.7643	4.72	19.78
11	Z-R-5	1.0000	0.9429	0.7496	5.71	20.50
12	Z-R-6	1.0000	0.9532	0.7787	4.68	18.31
13	Wako (Japan)	1.0000	0.9029	0.7299	9.71	19.15
14	Degussa (Japan)	1.0000	0.8897	0.7350	11.03	17.38

Table 3.5:Moisture content and water of hydration of flyash zeolite and standard zeolite

Sr. No	Name of zeolite	Si/Al ratio	Mass of air-dried zeolite (Grams)	Mass of oven-dried zeolite (Grams)	Mass of anhydrate zeolite (Grams)	Titration reading in ml for 25 ml sample				Cation exchange capacity Meq. / g	
						Fresh zeolite		Regenerated zeolite		Fresh zeolite	Regenerated zeolite
						Blank	Exchanged	Blank	Exchanged		
						Blank	Exchanged	Blank	Exchanged		
1	Z-A-3	2.54	1.0659	1.0000	0.8373	28.3	25.1	29.8	26.8	2.56	2.39
2	Z-R-3	1.73	1.0636	1.0000	0.7864	28.4	25.5	27.9	25.1	2.96	2.28
3	Z-R-1	1.60	1.0608	1.0000	0.8037	28.4	24.2	29.3	25.4	3.36	3.87
4	Z-R-6	1.50	1.0491	1.0000	0.8169	28.4	24.1	29.3	27.4	3.45	1.52
5	Z-A-2	1.50	1.0730	1.0000	0.7919	28.7	23.5	27.7	22.7	4.20	4.10
6	Z-A-6	1.35	1.0511	1.0000	0.7988	28.7	23.5	27.7	24.8	4.16	2.32
7	Z-A-1	1.24	1.0621	1.0000	0.8132	28.5	23.0	27.3	22.5	4.40	3.87
8	Z-R-2	1.00	1.0648	1.0000	0.8031	28.5	22.7	27.3	22.0	4.64	4.25
9	Z-R-4	1.00	1.0495	1.0000	0.8022	28.7	23.9	30.1	25.5	3.84	3.70
10	Z-A-4	1.00	1.0499	1.0000	0.8260	28.7	21.4	30.1	23.4	5.84	5.36
11	Z-R-5	1.00	1.0606	1.0000	0.7950	28.3	25.1	28.9	25.0	3.2	3.12
12	Wako Japan	1.00	1.1075	1.0000	0.8085	28.6	20.4	28.3	21.3	5.76	5.60
13	Degussa Japan	1.00	1.1235	1.0000	0.8262	28.4	23.2	27.7	21.6	4.96	4.80

Table 3.6: Cation exchange capacity of flyash zeolites and standard zeolites.

Sr.No	Name of zeolite	Si/Al ratio	Mass of air-dried sample in grams	Total NOx consumed in ml	MI of NOx consumed per gram of air-dry zeolite	% Nitrogen in nitrated zeolite	Molecular weight of one repeat unit	No. of equivalent of nitrogen per repeat unit
1	Z-A-3	2.54	1.0	900	900	3.85	446	1.22
2	Z-R-3	1.73	15.0	15,000	1000	3.85	182.6	0.50
3	Z-R-1	1.60	15.0	15,000	1000	3.85	244	0.67
4	Z-R-6	1.50	15.0	15,000	1000	3.85	188	0.52
5	Z-A-2	1.50	1.0	900	900	3.85	262	0.72
6	Z-A-6	1.35	15.0	15,000	1000	3.85	223	0.61
7	Z-A-1	1.24	1.0	900	900	3.85	179.6	0.49
8	Z-R-2	1.00	15.0	15,000	1000	3.85	142	0.39
9	Z-R-4	1.00	15.0	15,000	1000	3.85	248	0.68
10	Z-A-4	1.00	15.0	15,000	1000	3.85	142	0.38
11	Z-R-5	1.00	15.0	15,000	1000	3.85	248	0.68

Table 3.7: Details of the experimental conditions of nitration reactions and analysis of number of equivalents of nitrogen attached per repeat unit of flyash zeolite

Name of zeolite & JCPDS file No.	ds ₁ (%RI)	ds ₂ (%RI)	ds ₃ (%RI)	ds ₄ (%RI)	ds ₅ (%RI)	Σ RI	Percent crystallinity
Blank Z-A-4	12.7 (100)	3.00 (83.3)	3.75 (72.0)	3.32(63.1)	2.64 (60.2)	378.3	100 percent
JCPDS file No 11 - 590	12.3 (100)	2.99 (55.0)	3.71(50.0)	3.30(45.0)	2.63 (20.0)	270.0	
Nitrated Z-A-4	3.1 (100)	2.34 (04.0)	2.12(04.0)	1.93(25.0)	2.00 (06.0)	156.7	100 percent
JCPDS file No. 24 - 1047	3.2 (100)	2.31 (24.0)	2.13(15.67)	1.9(11.0)	1.95 (6.12)	139.0	

Table 3.8: The d-spacing and relative intensity values of XRD analysis of blank & nitrated flyash zeolite (A-4) and their most closely matching standard sodium aluminosilicate zeolite reported in JCPDS cards.

Sr. No	Name of zeolite	Si/Al ratio	Cation exchange capacity Meq. /g	Aminated zeolite			Quarternized zeolite		
				Mass of zeolite (Grams)	Mass of AgCl ppt. (Grams)	AEC in Meq. /g	Mass of zeolite (Grams)	Mass of AgCl ppt (Grams)	AEC in Meq. /g
1	Z-R-2	1.00	4.64	0.9982	0.2361	1.65	1.0010	0.4707	3.28
2	Z-A-4	1.00	5.84	1.0085	0.2491	1.72	1.0002	0.4445	3.10
3	Z-R-4	1.10	3.84	1.0028	0.2440	1.70	0.9987	0.4481	3.13
4	Z-R-5	1.00	3.20	0.9997	0.2580	1.80	0.9746	0.4876	3.49
5	Z-A-1	1.24	4.40	1.0098	0.2635	1.82	0.9831	0.3946	2.80
6	Z-A-6	1.35	4.16	0.9899	0.2767	1.95	0.9889	0.4207	3.32
7	Z-R-6	1.50	3.45	1.0005	0.3012	2.10	1.1003	0.5726	3.63
8	Z-A-2	1.50	4.20	1.0002	0.2868	2.00	0.9799	0.5169	3.68
9	Z-R-1	1.60	3.36	0.9989	0.2993	2.09	1.0001	0.5562	3.88
10	Z-R-3	1.73	2.96	1.0037	0.3065	2.13	1.0001	0.4287	2.99
11	Z-A-3	2.54	2.56	1.0000	0.3441	2.40	1.0006	0.5333	3.72

* All masses are expressed on oven dry basis.

- AEC: Anion exchange capacity of zeolite expressed in meq. / g of oven dry zeolite

Table 3.9: Anion exchange capacity of aminated and quarternized flyash zeolite.

Sr. No.	Name of silica	XRD analysis	BET surface area (m ² /g)	Pore volume (cc/g)	Particle size distribution			
					% Particle less than 4 μ m	% Particle less than 10 μ m	% Particle less than 40 μ m	Average size range (μ m)
1	Meso-Si-1	Amorphous	833.51	0.5315	6.90	19.98	94.62	21.0 – 32.0
2	Meso-Si-2	Amorphous	841.30	0.4974	9.08	26.28	95.33	19.6 – 31.0
3	Flyash Meso-Si	Amorphous	398.03	-	11.51	24.6	99.90	14.0 – 25.0

Table 3.10: The characterization of mesoporous silica synthesized from TEOS and Flyash mother liquor.

Chapter 4

Conclusion

We have synthesized the sodium aluminosilicate zeolite from flyash with varying Si/Al ratio. These zeolites are compared with standard sodium aluminosilicate zeolites reported in the JCPDS cards using the XRD analysis. This way the XRD was used for characterizing other flyash zeolites with respect to their crystallinity, molecular structure, crystal structure and the Si/Al ratio. These zeolites have further been characterized with respect to particle size, specific surface area, sorption capacity and the cation exchangeability. We have then modified these through gas phase nitration by NO_x and confirmed the Si- NO_2 bond through FTIR, ESCA, XRD and Elemental analysis of the modified and unmodified zeolite. We have proposed the mechanism of the nitration reaction of the flyash zeolite.

In the proposed mechanism, the Si-O bond at the aluminosilicate lattice is assumed to break in the presence of NO_x and gives Si^\bullet and SiO^\bullet radicals on the crystal structure along with the hydrogen and hydroxyl radicals by dissociation of water in the gas phase. The Si radical then combine with NO_2 (which is stable radical) after it diffuses from the bulk to give Si- NO_2 as well as with hydroxyl radical (which also diffuses from gas phase) to give Si-OH bonds. The formation of Si- NO_2 has been supported by FTIR, ESCA, XRD and Elemental analysis of the blank and the nitrated zeolite. It is found that due to this break in Si-O-Si bond in the crystal, the geometry of the zeolite after nitration changes from cubic (100 % crystalline) to monoclinic (100 % crystalline). These Si- NO_2 group has been reduced to Si- NH_2 group in the

zeolite through amination. The resultant amphoteric zeolite has excellent cation exchangeability, which is not affected by the nitration reaction. It is found that the cation exchangeability increases with decrease in the Si/Al ratio whereas the anion exchangeability is found to decrease. This is because the Al does not react with NO_x but forms an ionic bond with sodium. The Si-NH₂ bonds are found to react with dichloroethane like any organic molecule and after quarternization with trimethylamine, the anion exchange capacity is found to be doubled indicating that two molecules of the latter reacts with one amine group.

References

1. Chankya Misra, Crystalline zeolite and methods of preparation from amorphous silica particles, US Patent Number, 5,275,800, 1994.
2. A. K. Cheetham, G. Ferey and T. Loiseau, Open-framework inorganic materials, *Angew. Chem. Int. Ed.* 38, 3268-3292, 1999.
3. C.Freybardt, M. Tsapatsis, R.F. Lobo, M.E. Davis, High silica zeolite with a 14 tetrahedral atoms pore openings, *Nature*, 381, 295, 1996.
4. M. A. Camblor, M. J. Diaz-Cabanas, J.Perez-Pariente, An odd zeolite with pore openings of seven and nine tetrahedral atoms, *Angew. Chem. Int. Ed.*, 37, 2122, 1998.
5. J. Y. Ying, P.Mehnert and M.S.Wong, Synthesis and application of supramolecular templated mesoporous material, *Angew. Chem. Int. Ed.*, 38, 56-77, 1999.
6. J. S. Beck et al., Molecular or supramolecular templating: Defining the role of surfactant chemistry in the formation of MCM-41 and zeolite molecular sieves, *Studies in Surface Science and Catalysis*, 98, 15-16, 1998.
7. S. Inagaki et al., Novel mesoporous materials with a uniform distribution of organic group and inorganic oxides in their frameworks, *Journal of American Chemical Society*, 121, 9611-9614, 1999.
8. D.A.Loy, K. J. Shea, *Chem. Review*, 95 1431-1442, 1995.
9. L. Pauling, *The nature of the chemical bonds*, Cornell University Press Ithaca, 1960.

10. G. Bellussi, M. S. Rigutto, *Studies in Surface Science and Catalysis*, 85, 177-213, 1994.
11. A. Corma, M. T. Navarro, J. P. Pariente, Synthesis of an ultra large pore titanium silicates isomorphous to MCM-41 and its application as a catalyst for selective oxidation of hydrocarbon, *Journal of Chemical Society, Chemical Communication*, 147-148, 1994.
12. K. A. Koyano, T. Tatsumi, Synthesis of titanium containing mesoporous molecular sieve with a cubic structure, *Chemical Communication*, 145-146, 1996.
13. T.H. Chang, F. C. Leu, Synthesis and characterization of vanadium titanium silicates molecular sieve with MEL structure, *Zeolite*, 15, 496-500, 1995.
14. A. Tuel, Y.B. Taarit, Synthesis and catalytic properties of titanium-substituted silico-aluminophosphate. *Zeolite*, 14, 18-24, 1994.
15. W. Zhang, T. J. Pinnavaia, Catalytic hydroxylation of benzene over transition-metal substituted hexagonal mesoporous silicas, *Catalysis Letter*, 38, 261-265, 1996.
16. K. M. Reddy, I. Modrakovski, A. Sayari, Synthesis of mesoporous vanadium silicates molecular sieves, *Journal of Chemical Society, Chemical communication*, 1059-1060, 1994.
17. R. F. Parton, I. F. J. Vankelecom et al., An efficient mimic of cytochrome P-450 from a zeolite-encaged iron complex in polymer membrane, *Nature*, 370, 541-543, 1994.
18. A. V. Kucherov, A. A. Slinkin, G. K. Beyer, G. Borbely, *Zeolites*, 15, 431-438, 1995.

19. W. Zhang, J. Wang, P. T. Tanev, T. J. Pinnavaia, Catalytic hydroxylation of benzene over transition metal substituted hexagonal mesoporous silicas, Chemical Communication, 979-980, 1996.
20. D. Zhao, D. Goldfarb, Synthesis of mesoporous manganese silicates: Mn-MCM-41, Mn-MCM-48, Mn-MCM-L, Journal of Chemical Society Chemical Communication, 875-876, 1995.
21. P. Ratnasamy, R. Kumar, Process for the preparation of crystalline aluminophosphate catalyst, Catalysis Today, 9, 329-416, 1991.
22. A. Tuel, S. Gontier, Novel zirconium containing mesoporous silica for oxidation reaction in the liquid phase, Chemical Material, 8, 114-122, 1996.
23. B. Echchabed, A. Moen, D. Nicholson, L. Bonneviot, Modified MCM-48 mesoporous molecular sieves, Chemical Material, 9, 1716-1719, 1997.
24. J. A. Rossin, C. Saldarriaga, M. E. Davis, Zeolite, 7, 295-300, 1987.
25. S. J. Jong, S. Cheng, Reduction behavior and catalytic properties of cobalt containing ZSM-5 zeolite. Applied Catalysis A, 126, 51-66, 1995.
26. T. Inai, S. Iwamoto, K. Marsuba, Y. Tanaka, T. Yoshida, On the vital role of zeolitic matrix in catalysts for deNO_x reaction under conditions similar to diesel engine exhaust. Catalysis Today, 26, 23-32, 1995.
27. T. Inue, Novel catalytic function of metallosilicates exerted by isomorphous substitution, Studies in Surface Science and Catalysis, 83, 263-272, 1994.
28. L. Sierra, J. Patarin, C. Deroche, H. Gries, J. L. Guth, Room temperature synthesis of crystalline solid in the system ZnO-P₂O₅-R-H₂O, with R being an alkylamine or a alkyl ammonium ion, Studies in Surface Science and Catalysis, 84, 2237-2244, 1994.

29. G. R. Wang, X. Q. Wang, X. S. Wang, S. X. Yu, Synthesis and catalytic reaction of zirconium ZSM-5, *Studies in Surface Science and Catalysis*, 83, 67-74, 1994.
30. N. K. Mal, A. Bhaumik, V. Ramaswamy, A. A. Belhekar, A. V. Ramaswamy, Synthesis of Al-free Sn-containing molecular sieves of MFI, MEL and MTW types and their catalytic activity in oxidation reactions. *Studies in Surface Science and Catalysis*, 94, 317-324, 1995.
31. N. K. Mal, A. Bhaumik, V. Ramasewamy, S. Gonapathy, A. V. Ramaswamy, Synthesis of tin-silicate molecular sieve with MEL structure an their catalytic activity in oxidation reaction. *Applied Catalysis A*, 125, 233-245, 1995.
32. T. M. Abdel-Fattah, T. J. Pinnavaia, Tin substituted mesoporous silica molecular sieve (Sn-HMS): synthesis and properties as a heterogeneous catalyst for lactide ring opening polymerization, *Chemical Communication*, 665-666, 1996.
33. A. Bhaumik, S.G. Hegde, R. Kumar, Physicochemical characterization of a synthesis merlinoite (linde W type) zeolite containing Na, K, and Cr cations, *catalysis letter*, 35, 327-334, 1995.
34. L. Zhang, J. Y. Ying, Synthesis and characterization of mesoporous niobium doped silica molecular sieve. *AIChE Journal*, 43, 2793-2801, 1997.
35. S. Sayari, C. Danamah, I. L. Moudrakovski, Boron modified MCM-41 mesoporous molecular sieve, *Chemical Material*, 7, 813-815, 1995.
36. C. F. Cheng, H. He, W. Zou, J. Klinowski, J. A. S. Goncalves, L. F. Gladden, Synthesis and characterization of the gallosilicates mesoporous molecular sieve MCM-41, *Journal of Physical Chemistry*, 100, 390-396, 1996.

37. J. S. Beck et al. A new family of mesoporous molecular sieves prepared with liquid crystal templates, *Journal of American Chemical Society*, 114, 10834-10843, 1992.
38. S. Dai, M. S. Burleigh et al. *Angew Chem. Int. Ed*, 38, No 9, 1999.
39. C. Beck, H. Hartl And R. Hempelman, Covalent surface functionalization and self-organization of silica nanoparticles, *Angew. Chem. Int. Ed*, 38, No 9, 1999.
40. S. Liu, X. Ye, Y. Wu, *Catalysis Letter*, 36, 263-266, 1996.
41. P. Sutra, D. Brune et al, Preparation of MCM-41 type silica-bound manganese (III) schiff-base complexes, *Chemical Communication*, 2485-2486, 1996.
42. C. Liu, S. G. Li, W, Q. Pang, C. M. Che, Ruthenium porphyrin encapsulated in modified mesoporous molecular sieve MCM-41 for alkene oxidation, *Chemical Communication*, 65-66, 1997.
43. T. Maschmeyer, R. D. Oldroyd et al. Designing a solid catalyst for the selective low-temperature oxidation of cyclohexane to cyclohexanone, *Angew Chemical*, 109, 1713-1716, 1997.
44. Dr. S. Bhatia, *Zeolite: A Promising Catalyst*, Vol. 1, 20-22, 1987.
45. Isabel, Arends, R.A. Sheldon et al. Oxidation transformation of organic compounds mediated by redox molecular sieve, *Angew. Chem. Int. Ed. England*, 36, 1144-1163, 1997.
46. A. E. Greenberg, L. S. Clesceri, A. D. Eaton, *Standard methods for the examination of water and waste water*, 3-57, 18th edition, 1992.
47. *Powder Diffraction File Search Manual*, Published by International Central for Diffraction Data, Pennsylvania, USA, 1978.

48. A. E. Greenberg, L. S. Clesceri, A. D. Eaton, Standard Methods for the Examination of Water and Waste Water, page No. 454, 18th edition, 1992.
49. R.P.Wayne and G. Wilkinson, Advanced Inorganic chemistry, 5th Ed., John Wiley & Sons, 320 –325, 1992.
50. P.Warneck, Chemistry of the Natural Atmosphere, 1st Ed., Academic press, Sandiago, 1988.